4408 *Chem. Mater.* **2009,** *21,* 4408–4424
DOI:10.1021/cm900862v

CHEMISTRY OF MATERIALS
Article

Probing the Origin of Enhanced Stability of "$AlPO_4$" Nanoparticle Coated $LiCoO_2$ during Cycling to High Voltages: Combined XRD and XPS Studies

Yi-Chun Lu,[†] Azzam N. Mansour,[‡] Naoaki Yabuuchi,[†] and Yang Shao-Horn*,[†]

[†]*Massachusetts Institute of Technology, Cambridge, Massachusetts 02139, and* [‡]*Naval Surface Warfare Center, Carderock Division, West Bethesda, Maryland 20817-5700*

Received March 28, 2009. Revised Manuscript Received July 20, 2009

"$AlPO_4$"-coated $LiCoO_2$ was shown to exhibit markedly improved capacity retention and reduced impedance growth relative to bare "$LiCoO_2$" upon cycling to 4.7 V. Scanning electron microscopy imaging showed that the surfaces of the cycled bare "$LiCoO_2$" particles remained very smooth whereas there were many newly formed patches distributed on the surfaces of the cycled coated particles. X-ray powder diffraction analyses revealed that select peak broadening was observed for cycled bare electrodes suggesting that structural damage to Li_xCoO_2 was introduced upon cycling. In contrast, no apparent structural changes to Li_xCoO_2 were found for cycled coated electrodes. Pristine and cycled bare and "$AlPO_4$"-coated $LiCoO_2$ electrodes were studied by X-ray photoelectron spectroscopy. No significant change was detected in the surface chemistry of Co for cycled bare electrodes, but surface LiF and $Li_xPF_yO_z$ components were found to considerably increase during cycling, which led to partial surface coverage of Li_xCoO_2. A very small amount of Co-containing oxyfluoride species was detected on the cycled bare electrodes while considerable amounts of Co-containing and Al-containing fluorides and/or oxyfluorides and species such as $PF_x(OH)_y$ were found on the cycled coated electrodes, which completely covered the surfaces of the Li_xCoO_2 particles. The mechanism responsible for the enhanced cycling stability and reduced impedance of coated relative to bare electrodes is discussed in detail.

Introduction

Application of an oxide, phosphate, and fluoride such as ZrO_2,[1] Al_2O_3,[1−3] TiO_2,[1,4] $AlPO_4$,[5−12] and AlF_3[13] to the surfaces of lithium transition metal oxide particles such as $LiCoO_2$ has been shown to improve capacity retention upon cycling to high voltages. However, the origin in the performance improvement of surface-modified positive electrodes during electrochemical cycling is not well understood. Cho et al.[14,15] and Fey et al.[16,17] have first proposed that the oxide coating (e.g., Al_2O_3 and ZrO_2) can suppress phase transitions by constraining active particles against lattice parameter changes associated with lithium removal and insertion, which would reduce stresses and structural damage within individual particles and improve capacity retention during cycling. However, it is shown subsequently[5−12,18] that suppression of lattice expansion is not necessary to obtain improved cycling performance of "$AlPO_4$"- and oxide-coated $LiCoO_2$. Another school of thought is that coating materials[19] and/or processes involved in application of coating[18] modify the surfaces of active materials and surface reactions between active materials and the electrolyte and stabilize active materials upon cycling to high voltages. On one hand, several studies[20,21] have shown that the

*Corresponding author. E-mail: shaohorn@mit.edu. Telephone: 617 253-2259.

(1) Kim, Y. J.; Cho, J. P.; Kim, T. J.; Park, B. *J. Electrochem. Soc.* **2003**, *150*, A1723.
(2) Oh, S.; Lee, J. K.; Byun, D.; Cho, W. I.; Cho, B. W. *J. Power Sources* **2004**, *132*, 249.
(3) Cho, J.; Kim, Y. J.; Park, B. *Chem. Mater.* **2000**, *12*, 3788.
(4) Fey, G. T. K.; Lu, C. Z.; Huang, J. D.; Kumar, T. P.; Chang, Y. C. *J. Power Sources* **2005**, *146*, 65.
(5) Cho, J. *Electrochim. Acta* **2003**, *48*, 2807.
(6) Cho, J.; Kim, Y. W.; Kim, B.; Lee, J. G.; Park, B. *Angew. Chem., Int. Ed.* **2003**, *42*, 1618.
(7) Lee, J. G.; Kim, B.; Cho, J.; Kim, Y. W.; Park, B. *J. Electrochem. Soc.* **2004**, *151*, A801.
(8) Kim, B.; Lee, J. G.; Choi, M.; Cho, J.; Park, B. *J. Power Sources* **2004**, *126*, 190.
(9) Cho, J.; Lee, J. G.; Kim, B.; Kim, T. G.; Kim, J.; Park, B. *Electrochim. Acta* **2005**, *50*, 4182.
(10) Cho, J.; Kim, T. G.; Kim, C.; Lee, J. G.; Kim, Y. W.; Park, B. *J. Power Sources* **2005**, *146*, 58.
(11) Cho, J. P.; Kim, B.; Lee, J. G.; Kim, Y. W.; Park, B. *J. Electrochem. Soc.* **2005**, *152*, A32.
(12) Kim, J.; Noh, M.; Cho, J.; Kim, H.; Kim, K. B. *J. Electrochem. Soc.* **2005**, *152*, A1142.
(13) Sun, Y. K.; Cho, S. W.; Myung, S. T.; Amine, K.; Prakash, J. *Electrochim. Acta* **2007**, *53*, 1013.
(14) Cho, J. P.; Park, B. *J. Power Sources* **2001**, *92*, 35.
(15) Cho, J.; Kim, Y. J.; Park, B. *J. Electrochem. Soc.* **2001**, *148*, A1110.
(16) Fey, G. T. K.; Weng, Z. X.; Chen, J. G.; Lu, C. Z.; Kumar, T. P.; Naik, S. P.; Chiang, A. S. T.; Lee, D. C.; Lin, J. R. *J. Appl. Electrochem.* **2004**, *34*, 715.
(17) Fey, G. T.-K.; Yang, H.-Z.; Prem Kumar, T.; Naik, S. P.; Chiang, A. S. T.; Lee, D.-C.; Lin, J.-R. *J. Power Sources* **2004**, *132*, 172.
(18) Chen, Z. H.; Dahn, J. R. *Electrochem. Solid State Lett.* **2004**, *7*, A11.
(19) Bai, Y.; Liu, N.; Liu, J. Y.; Wang, Z. X.; Chen, L. Q. *Electrochem. Solid State Lett.* **2006**, *9*, A552.
(20) Myung, S. T.; Izumi, K.; Komaba, S.; Sun, Y. K.; Yashiro, H.; Kumagai, N. *Chem. Mater.* **2005**, *17*, 3695.
(21) Kim, J. S.; Johnson, C. S.; Vaughey, J. T.; Hackney, S. A.; Walz, K. A.; Zeltner, W. A.; Anderson, M. A.; Thackeray, M. M. *J. Electrochem. Soc.* **2004**, *151*, A1755.

 Published on Web 09/09/2009

coating particles not only serve as a physical barrier to reduce the corrosion of the active material by HF in the electrolyte (a common contaminant in $LiPF_6$-containing electrolyte[22]) and to decrease electrode impedance but also scavenge HF in the electrolyte by the formation of metal fluorides. This mechanism (referred to as the HF-scavenger model here) could explain many common observed effects of metal oxide coatings such as (1) suppression of the dissolution of transition metals in the lithium transition metal oxides;[1] (2) reducing the side reactions, which can result in less decomposition of active materials and electrolytes; and (3) reduction of HF generation in the electrolyte solution.[20,23] On the other hand, Wang and co-workers[19,24,25] have shown that Al_2O_3 or YPO_4 particles increase the acidity of the electrolyte rather than scavenge the HF in the electrolyte, which can corrode the insulating surface species on $LiCoO_2$ and thus reduce electrode impedance. This discrepancy in the working mechanism limits the optimization of processes to stabilize lithium transition metal oxide electrodes. For example, the first mechanism points to the fact that the thickness and the uniformity of the coating layer are critical to enhance cycling performance[20] while the second mechanism[19,24−26] suggests that it is not essential for the coating layer to be compact or to be on the surface of the active materials to reduce capacity loss during cycling. Understanding the origin in the enhancement mechanism associated with coating materials on the cycling performance is essential to develop strategies to increase the lifetime of lithium batteries.

There is a lack of fundamental understanding on the influence of coating on the surface composition and structure changes of lithium transition metal oxide particles during electrochemical cycling and aging. A number of inorganic and organic species have been detected or suggested on the surfaces of active particles during cycling or exposure to salt-containing electrolyte in the work of Aurbach et al.[22,27−32] Organic species such as $ROCO_2Li$ can be formed on the oxide surfaces due to nucleophilic reactions between oxide particles (negatively charged oxygen on the surface) and electrophilic alkyl carbonates in the solvents such as ethylene carbonate (EC) of the electrolyte.[27−30,32] In addition, LiF can form on cycled and aged Li_xCoO_2 in the $LiPF_6$-containing electrolyte as a result of chemical reactions between HF and $LiCoO_2$,[22] which can lead to considerable electrode impedance growth as LiF is very resistive to Li ion migration. It is of great interest to examine the effect of coating on the surface chemistry of Li_xCoO_2 electrodes, which could provide insights to the mechanism of enhanced cycling performance found for "$AlPO_4$"-coated $LiCoO_2$ electrodes. The effects of Al_2O_3 and $AlPO_4$ coating on the surface chemistry of Li_xCoO_2 electrodes cycled up to 4.4 V vs Li have been studied by XPS[33] in some detail. Although coating is shown to reduce Co deposits on the negative electrode, no significant change in the surface composition and chemical environment of cycled Li_xCoO_2 is noted with coating addition. Such lack of difference between the cycled coated and bare Li_xCoO_2 electrodes may be related to the relatively low upper cycling voltage limits of 4.2 and 4.4 V used in this study and to the fact that the electrodes were washed with dimethyl carbonate (DMC) prior to XPS analysis.[33] Our previous study[34] has shown that "$AlPO_4$"-coated $LiCoO_2$ particles, where Li_3PO_4 and $LiCo_{1-y}Al_yO_2$ with relatively high Al substitution levels are detected on active particles, exhibit significant enhancement in the capacitance retention upon cycling to 4.7 V in comparison to bare "$LiCoO_2$". In this study, we utilize synchrotron X-ray powder diffraction to probe the bulk changes of bare and "$AlPO_4$"-coated $LiCoO_2$ upon cycling to 4.7 V and use X-ray photoelectron spectroscopy (XPS) to probe the changes in the surface chemistry induced upon cycling. We here discuss structural and surface compositional differences found in discharged bare and coated electrodes after cycling to 4.7 V vs Li, from which a mechanism responsible for the enhancement in cycle life of "$AlPO_4$"-coated $LiCoO_2$ electrodes is proposed and tested.

Experimental Section

Bare "$LiCoO_2$" and "$AlPO_4$"-coated $LiCoO_2$ powder samples were prepared as described previously.[34] Bare "$LiCoO_2$" was prepared from stoichiometric amounts of Co_3O_4 and Li_2CO_3 heated at 1000 °C for 4 h in an oxygen stream. An $AlPO_4$−nanoparticle solution was prepared by slowly dissolving $Al(NO_3)_3 \cdot 9H_2O$ and $(NH_4)_2HPO_4$ in distilled water until a white $AlPO_4$−nanoparticle suspension was observed. The $AlPO_4$ nanoparticles with particle sizes in the range of 5−10 nm were amorphous, as determined by X-ray diffraction.[9] Bare "$LiCoO_2$" was added to this suspension and mixed thoroughly for 5 min. The slurry was dried in an oven at 120 °C for 6 h and heat-treated at 700 °C for 5 h, from which the "$AlPO_4$"-coated $LiCoO_2$ was obtained. The weight fraction of "$AlPO_4$" on $LiCoO_2$ is 1% after firing at 700 °C, as determined by inductively coupled plasma-mass spectroscopy (ICP-MS) (ICPS-1000IV, Shimadzu).

The reversible capacities and cycling stability of bare "$LiCoO_2$" and "$AlPO_4$"-coated $LiCoO_2$ composite electrodes

(22) Aurbach, D.; Markovsky, B.; Rodkin, A.; Levi, E.; Cohen, Y. S.; Kim, H. J.; Schmidt, M. *Electrochim. Acta* **2002**, *47*, 4291.
(23) Sun, Y. K.; Lee, Y. S.; Yoshio, M.; Amine, K. *Electrochem. Solid State Lett*. **2002**, *5*, A99.
(24) Liu, J. Y.; Liu, N.; Liu, D. T.; Bai, Y.; Shi, L. H.; Wang, Z. X.; Chen, L. Q.; Hennige, V.; Schuch, A. *J. Electrochem. Soc*. **2007**, *154*, A55.
(25) Bai, Y.; Yin, Y. F.; Liu, N.; Guo, B. K.; Shi, H.; Liu, J. Y.; Wang, Z. X.; Chen, L. Q. *J. Power Sources* **2007**, *174*, 328.
(26) Park, S. B.; Shin, H. C.; Lee, W.-G.; Cho, W. I.; Jang, H. *J. Power Sources* **2008**, *180*, 597.
(27) Aurbach, D.; Markovsky, B.; Levi, M. D.; Levi, E.; Schechter, A.; Moshkovich, M.; Cohen, Y. *J. Power Sources* **1999**, *82*, 95.
(28) Aurbach, D. *J. Power Sources* **2000**, *89*, 206.
(29) Aurbach, D.; Gamolsky, K.; Markovsky, B.; Salitra, G.; Gofer, Y.; Heider, U.; Oesten, R.; Schmidt, M. *J. Electrochem. Soc*. **2000**, *147*, 1322.
(30) Aurbach, D. *J. Power Sources* **2003**, *119*, 497.
(31) Aurbach, D.; Talyosef, Y.; Markovsky, B.; Markevich, E.; Zinigrad, E.; Asraf, L.; Gnanaraj, J. S.; Kim, H. J. *Electrochim. Acta* **2004**, *50*, 247.
(32) Aurbach, D.; Markovsky, B.; Salitra, G.; Markevich, E.; Talyossef, Y.; Koltypin, M.; Nazar, L.; Ellis, B.; Kovacheva, D. *J. Power Sources* **2007**, *165*, 491.
(33) Verdier, S.; El Ouatani, L.; Dedryvere, R.; Bonhomme, F.; Biensan, P.; Gonbeau, D. *J. Electrochem. Soc*. **2007**, *154*, A1088.
(34) Appapillai, A. T.; Mansour, A. N.; Cho, J.; Shao-Horn, Y. *Chem. Mater*. **2007**, *19*, 5748.

were measured by using a two-electrode lithium cell (Tomcell type TJ-AC). Preparation of composite electrodes has been described in detail elsewhere.[34] Lithium cells were constructed inside the glovebox using a lithium metal foil as the negative electrode and the composite positive electrode separated by two polypropylene microporous separators (Celgard 2500). The electrolyte used was 1 M $LiPF_6$ in a 1:1 volume ratio EC/DMC solvent (Kishida Chemical Corp). Assembled lithium cells were allowed to soak for 6−8 h prior to electrochemical testing on a Solartron 1470 battery testing unit. Cycling characteristics of bare "$LiCoO_2$" and "$AlPO_4$"-coated $LiCoO_2$ electrodes were compared for two testing conditions. The first test was performed at a C/5 rate (bare: 0.12 mA/cm^2, coated: 0.16 mA/cm^2) between voltage limits of 3.0 and 4.7 V vs Li for 30 cycles after the first charge/discharge measured at a C/10 rate. The C-rate was defined based on the theoretical capacity of $LiCoO_2$ (274 mA h/g) in this study. The second test condition included galvanostatic cycling at a C/5 rate (bare: 0.29 mA/cm^2, coated: 0.36 mA/cm^2) between voltage limits of 2.5 and 4.7 V vs Li for 20 cycles, during which holding at 4.7 V was imposed for 4 h each cycle. The cells were disassembled in an argon-filled glovebox (<5 ppm of H_2O and O_2), after which Li_xCoO_2 electrodes were extracted and stored in hermetically sealed containers in the glovebox. The samples were then transported in these argon-filled containers for XPS and X-ray diffraction analyses. The discharged bare and coated electrodes cycled under the second test condition were examined by (1) JEOL 6320FV field-emission scanning electron microscopy (SEM) to investigate the changes in the surface morphology, (2) synchrotron X-ray diffraction to show the changes in the bulk crystal structure of $LiCoO_2$, and (3) XPS to reveal the changes in the surface compositions and chemical environments induced upon cycling. It should be noted that there are 10 wt % of PVDF binder and 10 wt % of Super P carbon in all of the pristine and discharged bare and coated electrodes. Therefore, the intensity of the signals from the binder and conductive additive are relatively higher in this study.

Synchrotron radiation of BL02B2 at SPring-8 (Sayo-gun, Hyogo, Japan), equipped with a large Debye−Scherrer camera,[35] was used to collect X-ray diffraction data of the cycled electrode samples. The incident beam was adjusted to a wavelength of 0.5 Å by a Si(111) monochromator to minimize the absorption by the samples. The wavelength was calibrated to 0.5027 Å using a CeO_2 standard (S.G. $Fm\bar{3}m$, $a = 5.4111(1)$ Å). The diffraction patterns were collected in the 2θ-range of 0 to 75°. A few milligrams of each sample were placed in a Linderman capillary (0.5 mm in diameter and approximately 2 cm in height) during the measurement. X-ray diffraction data were recorded on an imaging plate for 20 min. Rietveld refinement analysis was performed using FullProf[36] in the 2θ-range of 10−45° (d-spacing of 2.87−0.65 Å).

The XPS spectra of bare "$LiCoO_2$" and "$AlPO_4$"-coated $LiCoO_2$ electrodes before and after cycling were measured using a Physical Electronics model 5400 X-ray photoelectron spectrometer. The samples were removed from the argon-filled containers, mounted onto a gold-coated sample holder, and transferred into the introduction chamber of the XPS spectrometer under ambient conditions in about 2 min. The introduction chamber was then immediately evacuated using a combination of roughing and turbomolecular pumps for about 10 to 15 min before transferring the sample to the XPS analysis chamber. The data were collected at room temperature using a nonmonochromatic Al Kα (1486.6 eV) X-ray source operating at 400 W (15 kV and 27 mA). The X-ray source is located at 54.7° relative to the analyzer axis. All samples were analyzed at an electron takeoff angle of 45° relative to the sample plane. It should be noted that the X-ray source and collection angle of 45° used in this experiment yield a sampling depth of ~5 nm for the O 1s photoemission line.[37] The samples were mounted onto a gold-coated sample holder with the aid of electrically conducting tabs and were placed into the introduction chamber which was evacuated using roughing and turbomolecular pumps for about 10−15 min before being transferred into the analysis chamber of the XPS instrument. Data collection proceeded when the analysis chamber pressure reached $\sim 2 \times 10^{-8}$ Torr. The size of the analysis area was set to a 1.1-mm-diameter spot. Survey spectra were collected at low resolution using analyzer pass energy of 89.45 eV, an increment of 0.5 eV/step, and an integration interval of 50 ms/step. The final spectrum consisted of the average of 20 cycles. Multiplex spectra of various photoemission lines were collected at medium resolution using an analyzer pass energy of 35.75 eV, an increment of 0.2 eV/step, and an integration interval of 50 ms/step. Data collection intervals were approximately 37 min for survey spectra and ~100−200 min for each set of multiplex spectra depending on sample composition. Depth profile analysis was made using 4 KeV Ar ions with a raster size of 4×4 mm^2. The sputtering was made in 1-min intervals for a total sputtering time of 10 min for the bare electrode after 20 cycles and 20 min for the coated electrode after 20 cycles. The Li 1s, C 1s, O 1s, F 1s, Al 2s, Al 2p, P 2p, and Co 2p photoemission lines were collected after each interval of sputtering at constant analyzer pass energy of 71.0 eV and an energy increment of 0.5 eV. The sputtering rate was calibrated using a 1000 Å SiO_2 film on a Si substrate and was found to be in the range of 35−40 Å of SiO_2 per minute.

The linearity of the spectrometer energy scale was calibrated using the Au $4f_{7/2}$ and Cu $2p_{3/2}$ photoemission lines of sputter-cleaned foils. The measured binding energies for these two lines were 83.93 and 932.59 eV, respectively, which compared well with the established values of 84.00 and 932.66 eV. The measured binding energies were shifted only by −0.07 eV with respect to the established values. To compensate for this small shift and sample charging effects, all spectra of powder samples were calibrated with the C 1s photoemission peak for adventitious hydrocarbons at 285.0 eV.[38] Spectra for the electrodes were calibrated with respect to the approximate average of the binding energies for carbon black and hydrocarbons at 284.6 eV since their C 1s spectra include contributions from carbon black and hydrocarbons. It should be mentioned that small differences in binding energy scale from sample to sample could arise due to inherent differences in binding energies of hydrocarbons present on different surfaces. The procedures for curve fitting analysis of photoemission lines are discussed in detail elsewhere.[34] The relative sensitivity factors for Li 1s, C 1s, O 1s, F 1s, Co $2p_{3/2}$, Al 2s, and P 2p photoemission lines were given as 0.028, 0.314, 0.733, 1.00, 2.113, 0.312, and 0.525, respectively. To identify the nature of the bonding environments for pristine and cycled bare and coated $LiCoO_2$ electrodes, a number of

(35) Nishibori, E.; Takata, M.; Kato, K.; Sakata, M.; Kubota, Y.; Aoyagi, S.; Kuroiwa, Y.; Yamakata, M.; Ikeda, N. *Nucl. Instrum. Methods Phys. Res., Sect. A* **2001**, *467−468*, 1045.
(36) Rodríguez-Carvajal, J. *Physica B* **1993**, *192*, 55.
(37) *Surface Analysis by Auger and X-Ray Photoelectron Spectroscopy*; Briggs, D., Grant, J. T., Eds.; IM Publications and Surface Spectra Limited.: Manchester, 2003.
(38) Ikeo, N.; Iijima, Y.; Nimura, N.; Sigematsu, M.; Tazawa, T.; Matsumoto, S.; Kojima, K.; Nagasawa, Y. *Handbook of X-ray Photoelectron Spectroscopy*; JEOL: Tokyo, 1991.

reference compounds, namely, aluminum phosphate ($AlPO_4$), layered O3 $LiAl_{0.1}Co_{0.9}O_2$, lithium carbonate (Li_2CO_3), gamma lithium phosphate (γ-Li_3PO_4), layered O3 lithium aluminum oxide ($LiAlO_2$), cobalt(II) fluoride (CoF_2), cobalt(III) fluoride (CoF_3), aluminum fluoride (AlF_3), lithium hexafluorophosphate ($LiPF_6$), Super P carbon powder, PVDF powder, and 50 wt % PVDF and 50 wt % super P carbon composite electrode were used as standards for comparison. The X-ray powder diffraction patterns of some of the reference samples are shown in the Supporting Information (Figure S1).

Results and Discussion

Electrochemical Characterization. The galvanostatic voltage profiles of lithium cells having bare "$LiCoO_2$" and "$AlPO_4$"-coated $LiCoO_2$ electrodes reveal that the coated electrodes exhibit higher capacity in comparison to the bare electrode upon cycling to 4.7 V vs Li, as shown in Figure 1. This finding is in good agreement with previous studies.[5−12,34] It should be noted that the cell polarization grew considerably upon cycling, having that of cycled "$AlPO_4$"-coated $LiCoO_2$ much smaller than that of cycled bare, as shown in Figures 1a,b, respectively. With a 4-h holding at 4.7 V, the polarization of bare and coated $LiCoO_2$ electrodes became larger than those tested without holding, as shown in Figure 1c,d, respectively. After cycling with 4.7 V holding, coated electrodes maintained greater capacity retention (~70% retention) in comparison to bare electrodes (~50% retention). It is hypothesized that smaller polarization and larger reversible capacity of coated electrodes relative to bare electrodes upon cycling to 4.7 V can be attributed to enhanced structural and surface stability of coated $LiCoO_2$ relative to bare, which will be examined in detail by SEM, synchrotron X-ray diffraction and XPS in the following sections.

Microstructure Characterization—SEM Imaging. SEM secondary electron images of bare and "$AlPO_4$"-coated $LiCoO_2$ particles, before and after 20 cycles to 4.7 V with holding, are compared in Figures 2a-d, respectively. Before cycling, the surfaces of the bare "$LiCoO_2$" particles appear to be fairly smooth, as shown in Figure 2a, whereas the surfaces of the "$AlPO_4$"-coated $LiCoO_2$ particles are rough, as shown in Figure 2b. Our previous observations[34] have shown that the coating thickness varies on the micrometer scale with variations in the range of 10−100 nm. Interestingly, the surfaces of the cycled bare "$LiCoO_2$" particles in the discharged state were found to remain smooth after 20 cycles (Figure 2c). In contrast, a large number of additional deposits were found on the surfaces of cycled coated $LiCoO_2$ particles (Figure 2d) to the original surface morphologies (Figure 2b). The chemical nature of these new deposits in the cycled coated electrodes will be discussed in the context of the XPS results.

Synchrotron Powder X-ray Diffraction Analysis. The changes in the bulk crystal structure of bare and coated Li_xCoO_2 electrodes before and after cycling to 4.7 V with holding were examined by synchrotron X-ray diffraction. Figure 3a,b shows highlighted synchrotron

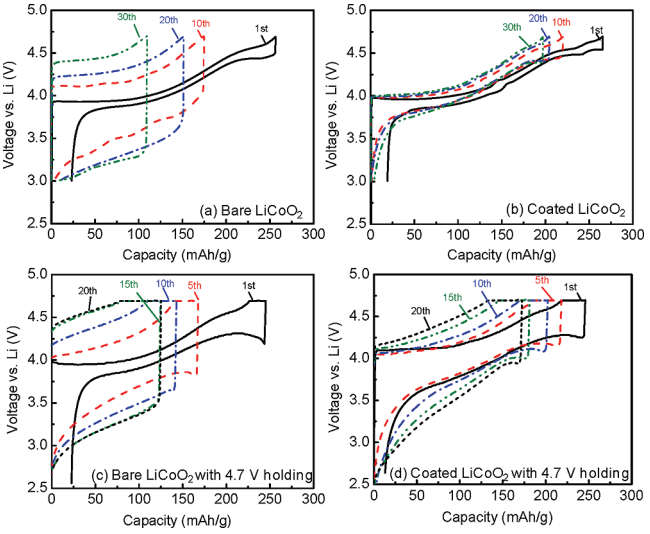

Figure 1. Voltage profiles of (a) bare "$LiCoO_2$" and (b) "$AlPO_4$"-coated $LiCoO_2$ during cycling between 3.0 and 4.7 V at a C/10 rate in the first cycle and a C/5 rate in the subsequent cycles. (c) bare "$LiCoO_2$" and (d) "$AlPO_4$"-coated $LiCoO_2$ during cycling between 2.5 and 4.7 V at a C/5 rate with holding at 4.7 V for 4 h. The cycled electrodes in the discharge state were used for XPS characterization.

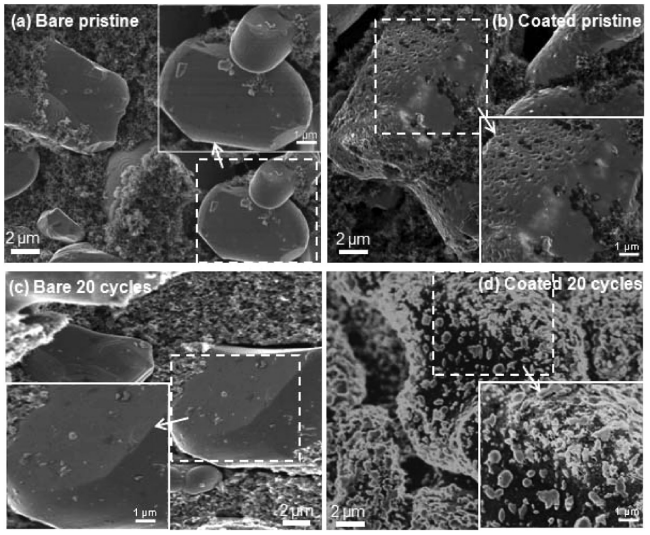

Figure 2. Scanning electron micrographs of (a) bare "$LiCoO_2$" pristine electrode and (b) "$AlPO_4$"-coated $LiCoO_2$ pristine electrode. The coated particles show pitted textures on the surface. (c) Bare "$LiCoO_2$" after 20 cycles to 4.7 V with holding and (d) "$AlPO_4$"-coated $LiCoO_2$ after 20 cycles to 4.7 V with holding. No apparent changes for the bare samples after cycling, whereas many newly formed patches were found on the surfaces of the coated particles after cycling.

X-ray diffraction patterns of pristine and cycled bare and coated electrodes in the discharged state, where Bragg reflections are indexed to a hexagonal unit cell with rhombohedral symmetry having space group $R\bar{3}m$. The crystallographic parameters of pristine and cycled, bare and coated $LiCoO_2$ in the rhombohedral symmetry were obtained from the Rietveld refinement of the diffraction data, as shown in Table 1. The lithium content in Li_xCoO_2 of cycled electrodes was estimated from the refined X-ray diffraction results and the open-circuit voltages (OCV) of the cells. We have previously shown that the coated $LiCoO_2$ exhibits a voltage plateau and a

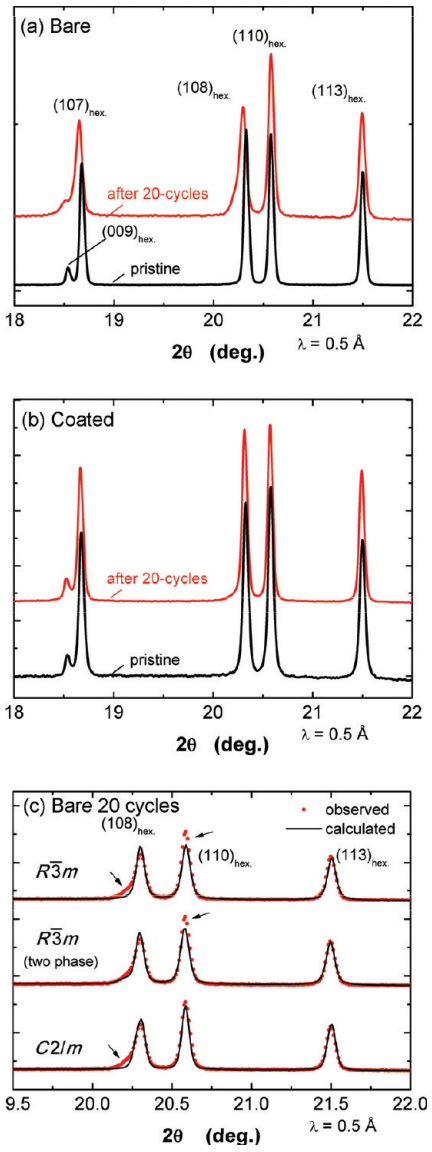

Figure 3. Synchrotron X-ray diffraction patterns, before and after cycling to 4.7 V with holding of (a) bare and (b) "$AlPO_4$"-coated $LiCoO_2$ electrodes. No apparent change was found for the coated electrode after 20 cycles, whereas peak broadening was noted for the bare sample after 20 cycles, indicating structural damage to Li_xCoO_2 upon cycling. (c) Comparison of experimental X-ray diffraction pattern of the bare "$LiCoO_2$" after 20 cycles with calculated patterns of the single-phase with space group $R\bar{3}m$, mixture of two $R\bar{3}m$ phases, and single-phase with space group $C2/m$.

two-phase reaction upon initial lithium deintercalation,[34] which is characteristic of stoichiometric $LiCoO_2$,[39−42] whereas bare "$LiCoO_2$" exhibits a slopping voltage profile and a single-phase reaction upon lithium deintercalation, which suggests that bare "$LiCoO_2$" is lithium overstoichiometric. The OCV result of the coated Li_xCoO_2 (Figure S2, Supporting Information) shows that the two-phase region starts from $x = \sim 0$ and ends at $x = \sim 0.75$ while that of the bare Li_xCoO_2 reveals a single-phase region in the same lithium compositional window. Neither changes in the crystallographic parameters of the hexagonal unit cell of cycled coated electrodes relative to the pristine electrode nor the appearance of a secondary phase of $Li_{0.75}CoO_2$ was detected. Therefore, the lithium content of the discharged coated $LiCoO_2$ after 20 cycles is estimated to be close to 1. In contrast, the unit cell dimension along the $c_{hex.}$ axis was increased slightly from the pristine (14.040 Å) to the cycled bare electrode in the discharged state (14.073 Å). Comparison with the lattice parameter changes of Li_xCoO_2 as a function of lithium content x reported by Levasseur et al.[43] suggest that the discharged bare electrode after 20 cycles has a lithium content of ~0.9 per unit formula.

It should be noted that the $(10l)_{hex.}$ peaks of the cycled bare Li_xCoO_2 were broadened selectively toward lower diffraction angles after 20 cycles, as shown in Figure 3a,c. For example, a peak shoulder toward the lower diffraction angles was very apparent for the $(108)_{hex.}$ reflection. Such broadening would not have been detectable using conventional laboratory diffractometers. In contrast, the peak profiles of all Bragg reflections for discharged coated $LiCoO_2$ remained unchanged after the cycling in Figure 3b. To examine and gain some insights into the origin of the observed peak broadening, the following structural analysis has been performed on the cycled bare "$LiCoO_2$". We applied two models, (1) a mixture of two $R\bar{3}m$ phases and (2) a monoclinic phase with space group $C2/m$. The observed and calculated intensities for these models are compared in Figure 3c. Although the observed peak shoulder can be simulated well using the two-phase model having the volume fraction of the secondary phase less than 10%, the observed intensity of the $(110)_{hex.}$ peak cannot be fitted satisfactorily, as shown in Figure 3c. On the other hand, the application of the monoclinic model with space group $C2/m$ was found to slightly improve the Rietveld refinement results in comparison to the single $R\bar{3}m$ phase, as shown in Table 1. However, these selectively broadened Bragg peaks could not be explained fully with the monoclinic phase, as shown in Figure 3c. We further discuss if proton insertion and/or oxygen loss is likely to give rise to the selective peak broadening. Several studies have shown that proton exchange for Li^+ in $LiCoO_2$ particles in acid,[44,45] where protons occupying prismatic sites instead of octahedral sites. can lead to shearing of oxygen lattice from ABCABC (O3 oxygen stacking) to ABBCCA (P3 oxygen stacking).[46] However, slabs with protons on the prismatic sites have smaller interslab distance relative to $LiCoO_2$, which would lead to selective peak broadening toward higher diffraction angles (not lower diffraction angles as observed in Figure 3). Therefore, the observed peak broadening is unlikely from proton exchange for Li in $LiCoO_2$. Although the origin of the peak broadening observed in cycled bare electrode is

(39) Menetrier, M.; Carlier, D.; Blangero, M.; Delmas, C. *Electrochem. Solid State Lett*. **2008**, *11*, A179.
(40) Menetrier, M.; Saadoune, I.; Levasseur, S.; Delmas, C. *J. Mater. Chem*. **1999**, *9*, 1135.
(41) Ohzuku, T.; Ueda, A. *J. Electrochem. Soc*. **1994**, *141*, 2972.
(42) Reimers, J. N.; Dahn, J. R. *J. Electrochem. Soc*. **1992**, *139*, 2091.
(43) Levasseur, S.; Menetrier, M.; Suard, E.; Delmas, C. *Solid State Ionics* **2000**, *128*, 11.
(44) Larcher, D.; Palacin, M. R.; Amatucci, G. G.; Tarascon, J. M. *J. Electrochem. Soc*. **1997**, *144*, 408.
(45) Benedek, R.; Thackeray, M. M.; van de Walle, A. *Chem. Mater*. **2008**, *20*, 5485.
(46) Butel, M.; Gautier, L.; Delmas, C. *Solid State Ionics* **1999**, *122*, 271.

Table 1. Crystallographic Parameters for the Pristine Bare and Coated Electrodes and the Cycled Bare and Coated Electrodes after 20 Cycles Obtained from the Rietveld Analysis

material			bare electrode	bare 20 cycles		coated electrode	coated 20 cycles
space group			$R\bar{3}m$	$R\bar{3}m$	$C2/m$	$R\bar{3}m$	$R\bar{3}m$
lattice constants	$a_{hex.}$ (Å)		2.81288(1)	2.81308(1)	$a_{mono.} = 4.8742(2)$ $b_{mono.} = 2.8130(1)$	2.81288(1)	2.81291(1)
	$c_{hex.}$ (Å)		14.0403(4)	14.0734(6)	$c_{mono.} = 4.9612(1)$ $\beta = 108.988(4)°$	14.0413(4)	14.0461(4)
Wyckoff position	3a site	Co (g)[a]	1.0	1.00	1.0 (2a site)	1.0	1.0
		B (Å^2)[a]	0.20	0.20	0.20	0.20	0.20
	3b site	Li (g)[a]	1.0	1.0	1.0 (2d site)	1.0	1.0
		B (Å^2)[a]	1.00	1.00	1.00	1.00	1.00
	6c site	O (g)[a]	1.0	1.0	1.0 (4i site)	1.0	1.0
		B (Å^2)	0.36(6)	0.55(9)	0.61 (8)	0.30(7)	0.41(6)
positional parameter for 6c site[b]			0.2603(4)	0.2608(4)	$x = 0.238(1)$ $z = 0.218(1)$	0.2603(4)	0.2601(4)
				Interatomic Distance			
Co−O (Å)			1.921	1.918	1.921	1.921	1.922
R_{wp} (%)			17.9	19.0	18.0	17.0	16.6
R_B (%)			6.18	9.29	9.00	6.99	5.81

[a] Not refined. [b] Oxygen positions are (0, 0, z) for $R\bar{3}m$ and (x, 0.5, z) for $C2/m$.

not fully understood, it is hypothesized that oxygen loss can give rise to the selective peak broadening observed for the cycled bare electrode. This hypothesis is supported by the fact that the isotropic displacement parameter of oxygen on the 6c site became larger in the cycled bare electrode than pristine bare when the occupancy of the oxygen was fixed, which indicates lowered local symmetry for MeO_6 octahedron and/or decreased oxygen occupancy at this site if the occupancy was allowed to vary. Further electron diffraction and high-resolution TEM imaging studies are needed to test this hypothesis.

XPS Results. *Pristine Bare and Coated Electrodes and Cycled Bare and Coated in the Discharged State*. The C 1s, Co 2p, and Co 2p depth profiles, F 1s, O 1s, and O 1s depth profiles, and P 2p and Al 2s spectra of pristine and discharged bare and coated $LiCoO_2$ electrodes after 1 and 20 cycles are shown in Figures 4−11, respectively. The Li 1s spectra are shown in Figure S3, Supporting Information. The XPS results reported here for pristine and cycled bare and coated electrodes were reproducible at least on three different electrodes in each case. It is noted that phase identification for complex electrode surfaces, based solely on XPS investigations, is not conclusive without further support from other techniques such as energy dispersive spectroscopy in scanning transmission electron microscopy at liquid nitrogen temperature and vibration spectroscopy. The reported phases, hereafter, were selected to represent, as closely as possible, the appropriate oxidation states and concentrations of various elements present in the surface region.

C 1s Region. The C 1s photoemission spectra of pristine and discharged electrodes after 1 and 20 cycles for bare and coated $LiCoO_2$ are shown in Figure 4. These spectra, except the one for the coated electrode after 20 cycles, are dominated by a contribution from Super P carbon black followed by a contribution from PVDF. The reference spectra of Super P carbon black, PVDF, and a composite electrode of 50 wt % PVDF and 50 wt % Super P carbon (Figure S4, Supporting Information) were used as a reference sample to deconvolute the spectra of composite electrodes. First, an asymmetric peak at 284.6 eV due to C—C bonding and a very broad peak with relatively lower intensity (5−10% of main peak)[47] at ∼290.5 eV due to the shakeup satellite structure can be attributed to carbon black. C—H bonds or adventitious hydrocarbons with binding energy around 285.0 eV are considered to have a relatively small contribution in the C 1s region shown in Figure 4a−e due to the fact that the first component shows similar characteristics to those of carbon black (highly asymmetric and narrow peak with a fwhm less than 1.5 eV). Second, a peak at ∼286.2 eV can be attributed to carbon atoms singly bound to oxygen (C—O)[48] and the CH_2 in PVDF.[33] Third, a peak near 287.6 eV can be related to carbon atoms bound to two oxygen atoms with two single bonds (O—C—O)[48] or bound to one oxygen with a double bond (C═O).[48,49] Fourth, a peak near 289.0 eV can be related to carbon bound to two oxygen atoms as in the carboxylic group (O—C═O).[48] Lastly, a peak located at 290.8 eV can be related to the CO_3 group in Li_2CO_3 (∼290.3 eV[34,50]) for pristine bare and coated $LiCoO_2$ particles and/or surface organic films consisting of species such as $ROCO_2Li$ (∼290.1 eV[51]) for cycled electrodes and carbon atoms bound to two fluorine atoms (CF_2 in PVDF). The amounts of oxidized carbon species slightly increased relative to aliphatic carbon (the 284.6 eV component) upon cycling of bare electrodes. In contrast, the contribution from carbon black at 284.6 eV decreased significantly in the coated electrode after 20 cycles relative to the pristine coated electrode. Instead a relatively broader

(47) *Surface Analysis by Auger and X-Ray Photoelectron Spectroscopy*; Briggs, D.; Grant, J. T., Eds.; IM Publications and SurfaceSpectra Limited.: Manchester, 2003.
(48) Ago, H.; Kugler, T.; Cacialli, F.; Salaneck, W. R.; Shaffer, M. S. P.; Windle, A. H.; Friend, R. H. *J. Phys. Chem. B* **1999**, *103*, 8116.
(49) Kozlowski, C.; Sherwood, P. M. A. *J. Chem. Soc., Faraday Trans. I* **1985**, *81*, 2745.
(50) Clemencon, A.; Appapillai, A. T.; Kumar, S.; Shao-Horn, Y. *Electrochim. Acta* **2007**, *52*, 4572.
(51) Dedryvere, R.; Gireaud, L.; Grugeon, S.; Laruelle, S.; Tarascon, J. M.; Gonbeau, D. *J. Phys. Chem. B* **2005**, *109*, 15868.

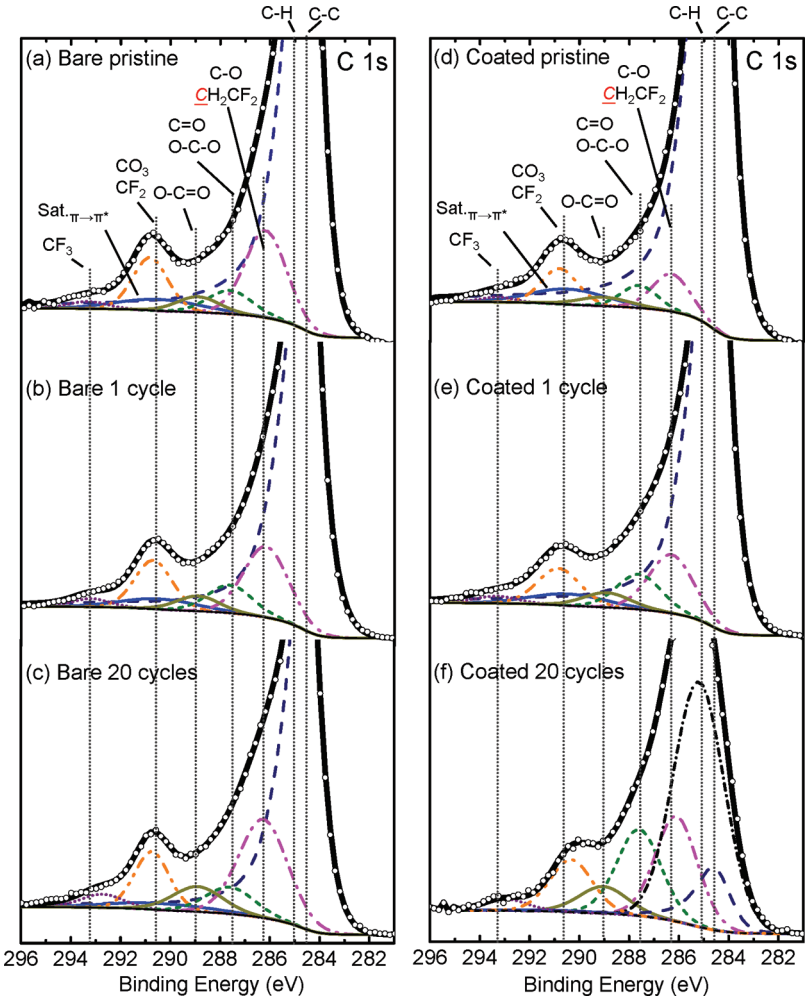

Figure 4. XPS spectra of the C 1s photoemission line for bare "$LiCoO_2$" in the condition of (a) pristine electrode, (b) after 1 cycle, and (c) after 20 cycles, and "$AlPO_4$"-coated $LiCoO_2$ in the condition of (d) pristine electrode, (e) after 1 cycle, and (f) after 20 cycles.

peak (fwhm of ~2.38 eV) near 285.0 eV was clearly recognized, which can be attributed to adventitious hydrocarbon. The significant decrease in the carbon black signal and the dominance of the hydrocarbon signal indicates that the surface film developed on the coated electrode after 20 cycles is much thicker than for the bare electrodes.

Co 2p Region. The Co 2p photoemission spectra of pristine and discharged electrodes after 1 and 20 cycles for bare and coated $LiCoO_2$ are shown in Figure 5. The spectra of pristine bare and coated electrodes reveal a $2p_{3/2}$ peak and a $2p_{1/2}$ peak at ~780 eV and ~795 eV, respectively. Shake-up satellite peaks for each line are located at ~9.7 eV higher relative to the main component. The locations and line shapes of the main peaks and their satellites of pristine electrodes indicate that cobalt ions are in the trivalent state.[52] The Co 2p spectra of cycled bare electrodes after 1 and 20 cycles were found similar to those of pristine bare "$LiCoO_2$" indicating that there was no apparent change in the Co oxidation state after cycling. In contrast, the Co 2p spectrum for the discharged coated electrode after 20 cycles is considerably different from that of the pristine coated electrode. First, the binding energy of the Co $2p_{3/2}$ line shifts from 780.4 eV for the pristine coated electrode to ~783.1 eV for the coated electrode after 20 cycles. Second, the spectrum of the coated electrode after 20 cycles displays an intense satellite structure at ~5.2 eV higher relative to the ~783.1 eV peak. The higher binding energy for the discharged coated electrode after 20 cycles relative to that of pristine coated electrode and the intense satellite structure with a 5.2 eV shift higher relative to the main peak can be attributed to Co bound to fluorine atoms, which indicates the formation of Co-containing fluoride and/or oxyfluoride species. This assignment was confirmed by the similarity in the Co 2p spectra between the discharged coated electrodes and a CoF_2 powder reference, which is shown in Figure 5f.

Figure 6 shows the Co 2p photoemission spectra of discharged bare and coated electrodes after 20 cycles as a function of sputtering time. For the discharged bare electrode, only small changes were found in the shakeup structure upon sputtering, where the increased shakeup intensities could be attributed to the formation of CoO by the reduction of the Ar beam during sputtering.[53] This

(52) Dupin, J. C.; Gonbeau, D.; Benqlilou-Moudden, H.; Vinatier, P.; Levasseur, A. *Thin Solid Films* **2001**, *384*, 23.

(53) Hagelin-Weaver, H. A. E.; Hoflund, G. B.; Minahan, D. M.; Salaita, G. N. *Appl. Surf. Sci.* **2004**, *235*, 420.

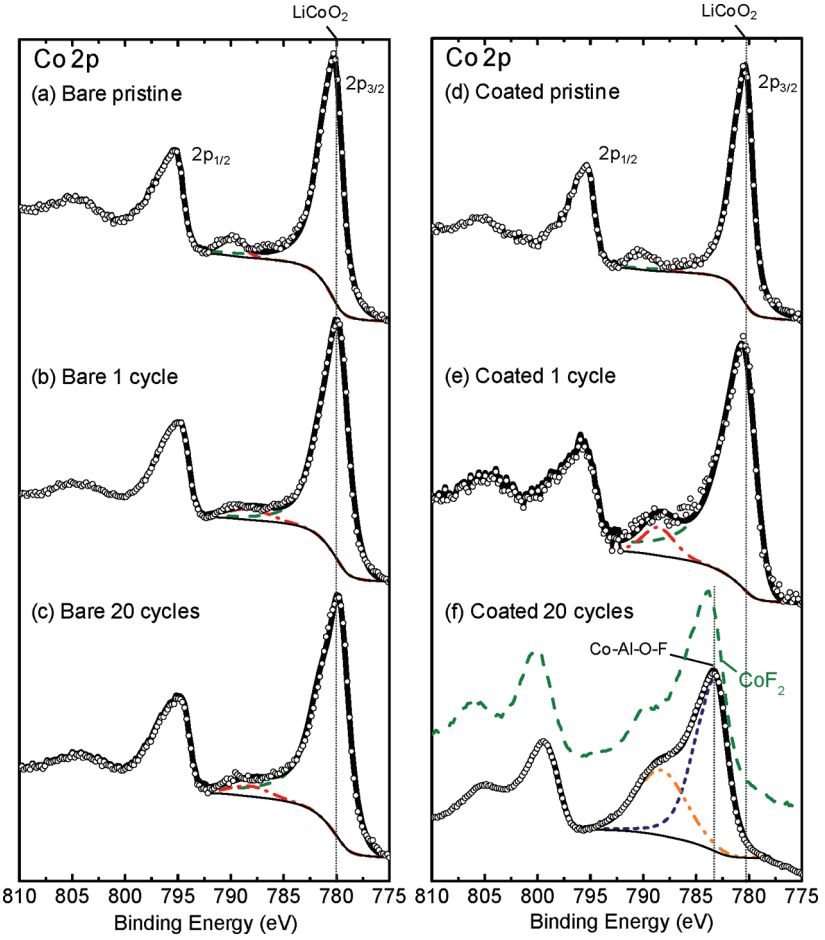

Figure 5. XPS spectra of the Co 2p photoemission line for (a) pristine bare "$LiCoO_2$" electrode, (b) after 1 cycle, and (c) after 20 cycles, and (d) pristine "$AlPO_4$"-coated $LiCoO_2$ electrode, (e) after 1 cycle, and (f) after 20 cycles.

observation suggests that there is no detectable difference in the cobalt valence state between the surface and bulk of cycled bare electrodes in the discharge state. On the other hand, the intensity of the higher binding energy component observed for the discharged coated electrode, which was attributed to Co bound to fluorine atoms, decreased with increasing sputtering time. The presence of Co-containing fluoride and/or oxyfluoride species can be related to the additional patches revealed by SEM on the surfaces of coated $LiCoO_2$ after cycling (Figure 2). The intensity of a lower binding energy peak near 779.5 eV, which corresponds to the Co^{3+} in $LiCoO_2$, became visible after only 1 min of sputtering, and its intensity increased with sputtering time. This result further supports the hypothesis that Co-containing fluoride and/or oxyfluoride species covers the surface of discharged coated Li_xCoO_2 after cycling to 4.7 V. Although how these fluoride and/or oxyfluoride species are formed on coated Li_xCoO_2 during cycling is not understood, it is interesting to mention that Markovsky et al.[54] have shown that adding Co^{2+} ions in the electrolyte leads to the formation of cobalt fluorides on the surface of Li_xCoO_2 cycled and aged in the $LiPF_6$-containing electrolyte.

An estimate for lithium content and subsequently the valence state of Co in the discharged state of Li_xCoO_2 can be made from the area of the satellite peak relative to that of the of Co 3p main line following the procedure reported by Daheron et al.[55] On this basis,[55] the discharged bare electrode after 20 cycles has a lithium content of ~0.9 per unit formula (Figure S5, Supporting Information), which is in agreement with the estimation from the synchrotron X-ray diffraction and OCV results discussed earlier in this paper. As the surface of discharged coated electrode after 20 cycles was covered largely by Co-containing fluoride and/or oxyfluoride species, this method is not appropriate to estimate the cobalt valence state in this case. It should be noted that we find no evidence for the presence of Co_3O_4 on the surface of cycled $LiCoO_2$ as suggested by previous studies[24,32] as broadening of the Co $2p_{3/2}$ line and shakeup structure expected for Co_3O_4 with Co^{2+} and Co^{3+}[56] relative to $LiCoO_2$ were not observed in this work. This result is in agreement with previous XPS findings of electrochemically deintercalated Li_xCoO_2 (x varies from 1 to 0)[55] and Li_xCoO_2 cycled to 4.4 V.[33] In addition, we find no

(54) Markovsky, B.; Rodkin, A.; Salitra, G.; Talyosef, Y.; Aurbach, D.; Kim, H. J. *J. Electrochem. Soc.* **2004**, *151*, A1068.
(55) Daheron, L.; Dedryvere, R.; Martinez, H.; Menetrier, M.; Denage, C.; Delmas, C.; Gonbeau, D. *Chem. Mater.* **2008**, *20*, 583.
(56) van Elp, J.; Wieland, J. L.; Eskes, H.; Kuiper, P.; Sawatzky, G. A.; de Groot, F. M. F.; Turner, T. S. *Phys. Rev. B* **1991**, *44*, 6090.

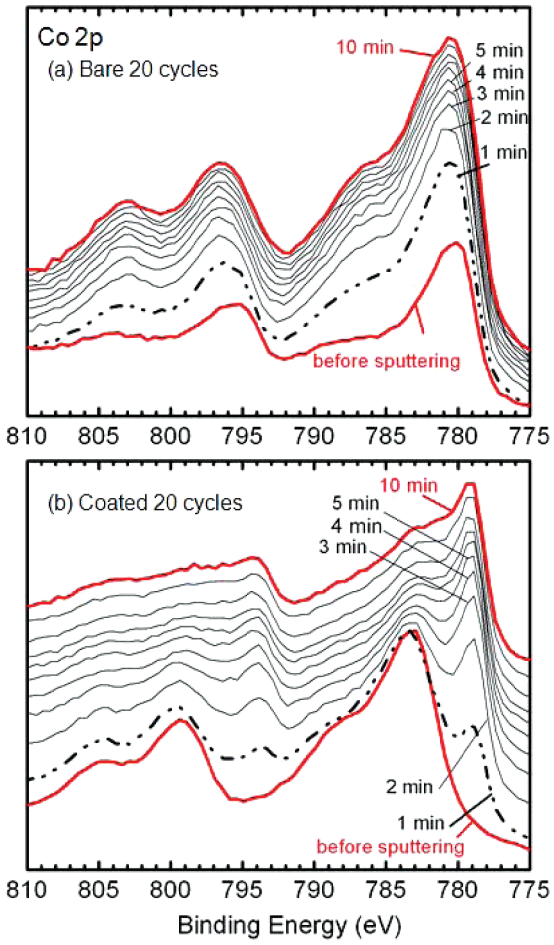

Figure 6. XPS depth profiles of the Co 2p photoemission line for (a) bare "$LiCoO_2$" after 20 cycles and (b) "$AlPO_4$"-coated $LiCoO_2$ after 20 cycles.

evidence for the presence of surface CoO or $Co(OH)_2$ for pristine and cycled bare and coated electrodes. The Co 2p binding energies for both CoO and $Co(OH)_2$ (XPS reference samples used in this study) are significantly lower than those of CoF_2 while their characteristic shakeup structures is much more intense than that of $LiCoO_2$ and are also shifted only by 7.0 and 6.1 eV, respectively, relative to the main line, which are significantly less than the 10 eV shift in the case of $LiCoO_2$.

F 1s Region. The F 1s photoemission spectra of pristine and discharged electrodes after 1 and 20 cycles for bare and coated $LiCoO_2$ are shown in Figure 7. The F 1s spectra of pristine bare (Figure 7a) and coated (Figure 7d) electrodes were deconvoluted into two components. An intense component at 688.0 eV is assigned to fluorine atoms in PVDF. This assignment is in good agreement with the F 1s binding energy of a reference sample having a mixture of PVDF and carbon (Figure S6a, Supporting Information). A weak component was found around 685.0 eV, which could be attributed to LiF (685.0 eV[33]). It is hypothesized that HF can be generated via a dehydrofluoination reaction in the PVDF binder and then react with $LiCoO_2$ or Li_2CO_3 to form LiF.[57]

(57) Edström, K.; Gustafsson, T.; Thomas, J. O. *Electrochim. Acta* **2004**, *50*, 397.

For the bare electrodes after 1 and 20 cycles and the coated electrode after 1 cycle, the F 1s spectra were deconvoluted into three components at ~688.0 eV, ~686.6 eV, and ~685.5 eV. The high-energy component at 688.0 eV can be attributed to PVDF (~688.0 eV) and $LiPF_6$ (~688.5 eV confirmed by a reference sample in this study). The intermediate-energy component at ~686.6 eV can be attributed to $LiPF_6$ degradation intermediates such as $Li_xPF_yO_z$.[33] It should be noted that this peak may include a contribution from $LiPF_6$ degradation products due to X-ray exposure during the XPS measurements. The low-energy component at ~685.5 eV can be attributed to LiF and other metal fluorides[54] and/or oxyfluoride species. For the coated electrode after 20 cycles, the F 1s spectrum was deconvoluted into two components. The component at 686.0 eV is assigned to the fluorine atoms in the form of Co-containing fluoride and/or oxyfluoride species. This assignment is consistent with the observed F 1s binding energy of 686.0 eV for a CoF_2 reference sample in this study. The high binding energy component of the F 1s line (688.5 eV), which contributes ~26.8 atom % to the composition, cannot be attributed fully to $LiPF_6$ and PVDF. On the basis of the composition and binding energy considerations, it is believed that this component likely includes contributions from PF_xO_y (e.g., OPF_3 and O_2PF) and/or $PF_x(OH)_y$ (e.g., $(OH)PF_4$, $(OH)_2PF_3$, $(OH)_3PF_2$, or $(OH)_4PF$). However, the F 1s binding energy reported for PF_xO_y ($LiPF_6$ decomposition products such as POF_3) is ~687 eV, its binding energy can be higher if the oxygen also binds to a hydrogen atom. Therefore, $PF_x(OH)_y$ appears to be a better candidate. In addition, a small amount of HF left on the surface cannot be excluded. However, since XPS cannot detect H, definitive confirmation of HF cannot be made. Detailed comparisons of surface chemical compositions of different species would be discussed in details in a later section.

O 1s Region. The O 1s photoemission spectra of the pristine and discharged electrodes after 1 and 20 cycles for bare and coated $LiCoO_2$ are shown in Figure 8. The spectra of pristine bare and coated electrodes consist of three components. First, the low-energy peak at ~529.7 eV can be attributed to lattice O^{2-} ions in the O3 layered $LiCoO_2$ structure. The second peak at ~532.0 eV can be attributed to surface defects associated with oxygen oxidation states less negative than O^{2-} ions[52,58] and more covalent Co−O bonds[59] on the "$LiCoO_2$" particle surface. In addition, the oxygen atoms in Li_2CO_3 (532.1 eV[34]) and oxygen atoms doubly bound to carbon atoms (532.0 eV) should also be considered in this component. A contribution from Li_3PO_4 (~531.6 eV[34]), which is present on the surface of pristine "$AlPO_4$"-coated $LiCoO_2$,[34] was also considered. The third component at 533.5 eV can be related to oxygen bound to carbon with a single bond as in ester groups.[49,60]

(58) Dupin, J. C.; Gonbeau, D.; Martin-Litas, I.; Vinatier, P.; Levasseur, A. *J. Electron. Spectrosc. Relat. Phenom.* **2001**, *120*, 55.
(59) Alcantara, R.; Ortiz, G. F.; Lavela, P.; Tirado, J. L.; Jaegermann, W.; Thissen, A. *J. Electroanal. Chem.* **2005**, *584*, 147.
(60) Zielke, U.; Hüttinger, K. J.; Hoffman, W. P. *Carbon* **1996**, *34*, 983.

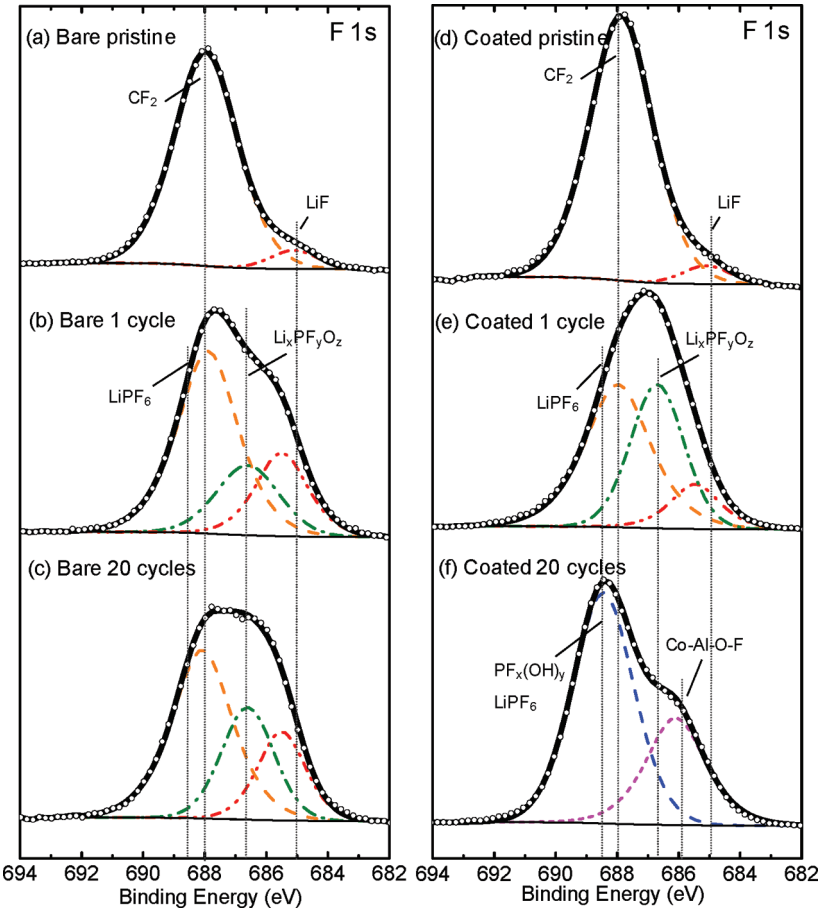

Figure 7. XPS spectra of the F 1s photoemission line for bare "$LiCoO_2$" in the condition of (a) pristine electrode, (b) after 1 cycle, and (c) after 20 cycles, and "$AlPO_4$"-coated $LiCoO_2$ in the condition of (d) pristine electrode, (e) after 1 cycle, and (f) after 20 cycles.

For the discharged bare electrodes, a peak near 531.0 eV appeared after 1 cycle and its intensity decreased after 20 cycles. This component can be related to metal hydroxide groups such as $Co(OH)_2$ (530.8 eV[61]) or LiOH (531.1 eV[61]). However, the Co environment in $Co(OH)_2$ was excluded since the Co 2p region for the discharged bare electrodes clearly show that the cobalt ions remained in the trivalent state.[52] Therefore, the oxygen component at 531.0 eV is likely due to LiOH, which could be formed by the reaction of OH^- (due to trace amount of water in the electrolyte) with Li^+ on the particle surface.[62] Upon cycling of bare electrode to 20 cycles, the carbonates species, which could develop from reactions between Li_xCO_2 and the electrolyte, were found to increase, as evidenced by the increased peak intensities at 532.0 eV (Li_2CO_3 and oxygen atoms forming a double bond with the carbon in Li alkyl carbonates $ROCO_2Li$[51]) and at ~533.5 eV (oxygen atoms forming a single bond with the carbon in Li alkyl carbonates $ROCO_2Li$,[51] $OP(OR)_3$,[33] and polycarbonate-type compounds[33]). A peak at very high binding energy of ~534.6 eV, which appeared after 20 cycles, was attributed to the oxygen atoms in fluorophosphate intermediates, namely, $Li_xPF_yO_z$.[63]

For the cycled coated electrodes, a peak at ~532.8 eV grew upon cycling and became dominant after 20 cycles, as shown in Figure 8e,f. This peak cannot be assigned to Li_2CO_3 as the binding energy of this component is not in good agreement with that of Li_2CO_3 and the two contributions of lithium alkyl carbonates,[51] and there are not enough oxidized carbon atoms to account for all of the oxygen atoms in the form of carbonates. As the O 1s binding energies of metal oxyfluoride species such as Al−O−F (~532.7 eV)[64] and Si_xOF_y (532.9 eV)[65] are close to 532.8 eV, the formation of $(OH)_yPF_x$ like species such as $(OH)PF_4$, $(OH)_2PF_3$, $(OH)_3PF_2$, or $(OH)_4PF$ is likely to occur on the surface of the cycled coated electrodes. However, based on the surface composition analysis, $(OH)_2PF_3$ appears to be the most likely candidate. The O 1s line of the coated electrode after 20 cycles is ~532.8 eV. It is reasonable to speculate that $PF_x(OH)_y$ has O 1s binding energy higher than pure hydroxides (typically in the range of 531.0−531.5 eV) as the presence of fluorine can increase its binding energy. For example, the binding energy of the O 1s line increased from 531.5 eV for $Al(OH)_3$ to 533.0 eV for $Al(OH)_{0.7}F_{2.3}$.[66] It should be noted that the

(61) Dupin, J.-C.; Gonbeau, D.; Vinatier, P.; Levasseur, A. *Phys. Chem. Chem. Phys.* **2000**, *2*, 1319.
(62) Liu, H. S.; Zhang, Z. R.; Gong, Z. L.; Yang, Y. *Electrochem. Solid State Lett.* **2004**, *7*, A190.
(63) Bryngelsson, H.; Stjerndahl, M.; Gustafsson, T.; Edstrom, K. *J. Power Sources* **2007**, *174*, 970.
(64) Miller, A. C.; McCluskey, F. P.; Taylor, J. A. *J. Vac. Sci. Technol. A* **1991**, *9*, 1461.
(65) Thomas, J. H.; Maa, J. S. *Appl. Phys. Lett.* **1983**, *43*, 859.
(66) Böse, O.; Kemnitz, E.; Lippitz, A.; Unger, W. E. S. *J. Anal. Chem.* **1997**, *358*, 175.

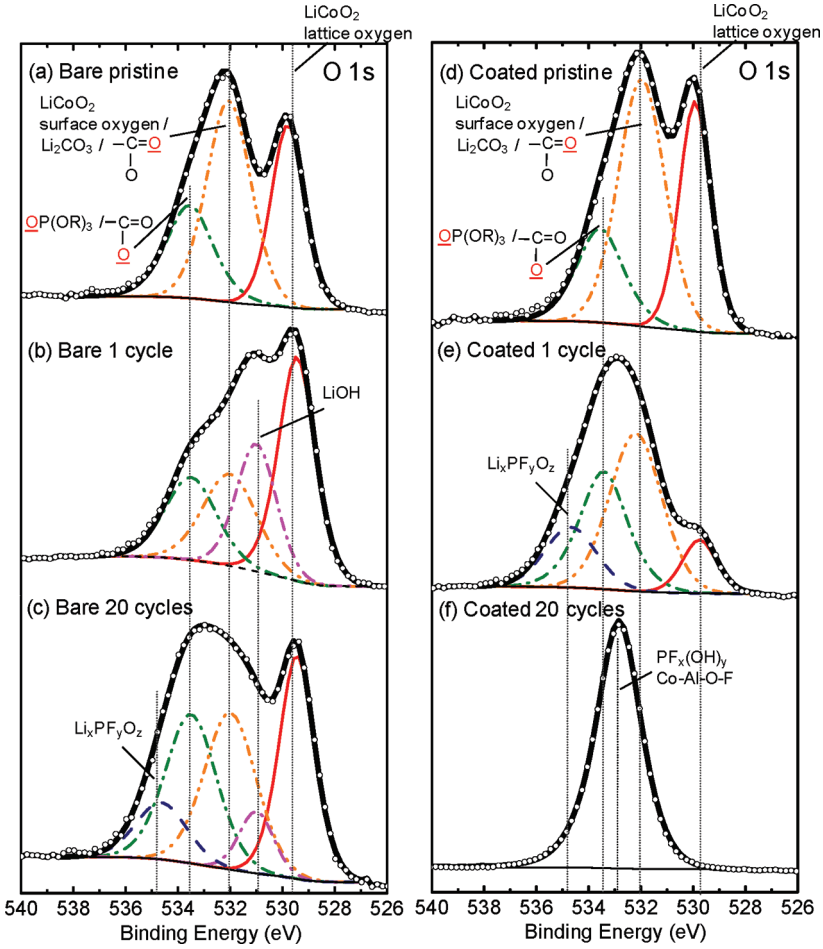

Figure 8. XPS spectra of the O 1s photoemission line for bare "$LiCoO_2$" in the condition of (a) pristine electrode, (b) after 1 cycle, and (c) after 20 cycles and "$AlPO_4$"-coated $LiCoO_2$ in the condition of (d) pristine electrode, (e) after 1 cycle, and (f) after 20 cycles.

peak corresponding to lattice oxygen in $LiCoO_2$ at ~529.6 eV is no longer detectable in the spectrum for the discharged coated electrode after 20 cycles (Figure 8f) while it is visible in the spectrum for the discharged bare electrodes after 20 cycles (Figure 8c). The absence of lattice oxygen and the significant reduction in the intensity of the carbon black signal for the coated electrode after 20 cycles are consistent with the formation of a surface film covering the precycled surface.

Figure 9 shows the O 1s photoemission spectra for the discharged bare and coated electrodes after 20 cycles as a function of sputtering time. For the discharged bare electrode, the intensity of components in the energy range from ~531 eV to ~534 eV decreased relative to that of the lattice O^{2-} component upon sputtering and was diminished after 3 min of sputtering. Similarly, the intensity of the surface oxygen peak of the discharged coated electrode decreased relative to that of lattice O^{2-} peak with sputtering time but remained visible after 10 min of sputtering. This observation further confirms that the surface film developed on the discharged coated electrode after 20 cycles is considerably thicker than that on the discharged bare electrode.

P 2p Region. The P 2p photoemission spectra of pristine and discharged electrodes after 1 and 20 cycles for bare and coated $LiCoO_2$ are shown in Figure 10. The spectra for the discharged bare electrodes after 1 cycle and 20 cycles show three contributions with the following binding energies: (1) ~133.5−134 eV, which can be assigned to phosphate species such as $OP(OR)_3$[33] resulting from degradation of $LiPF_6$; (2) ~136 eV, which can be attributed to $Li_xPF_yO_z$;[33] and (3) ~137.8 eV, which can be attributed to the $LiPF_6$ salt (~138 eV in the reference sample used in this study) in the electrolyte. The amounts of degradation products were found to grow with cycling. For the pristine coated electrode, the spectrum shows a single peak at 134.3 eV (Figure 10c), which can be attributed to Li_3PO_4 as reported previously.[34] In addition to Li_3PO_4, the spectrum of the discharged coated electrode after 1 cycle (Figure 10d) was fitted with three components similar to those found in the cycled bare electrodes. After 20 cycles, the XPS P 2p signal of the discharged coated electrode can be attributed to a minor component from $LiPF_6$ and a major component from species such as $PF_x(OH)_y$, which is supported by the fact that the binding energy of the P 2p line for the coated electrode after 20 cycles is close to that reported for $OPCl_3$ (135.9 eV[67]). The Li_3PO_4 component was no longer visible, which could be revealed after 10 min of sputtering (not shown). This observation suggests that some Li_3PO_4

(67) Fluck, E.; Weber, D. *Z. Naturforsch.* **1974**, *29B*, 603.

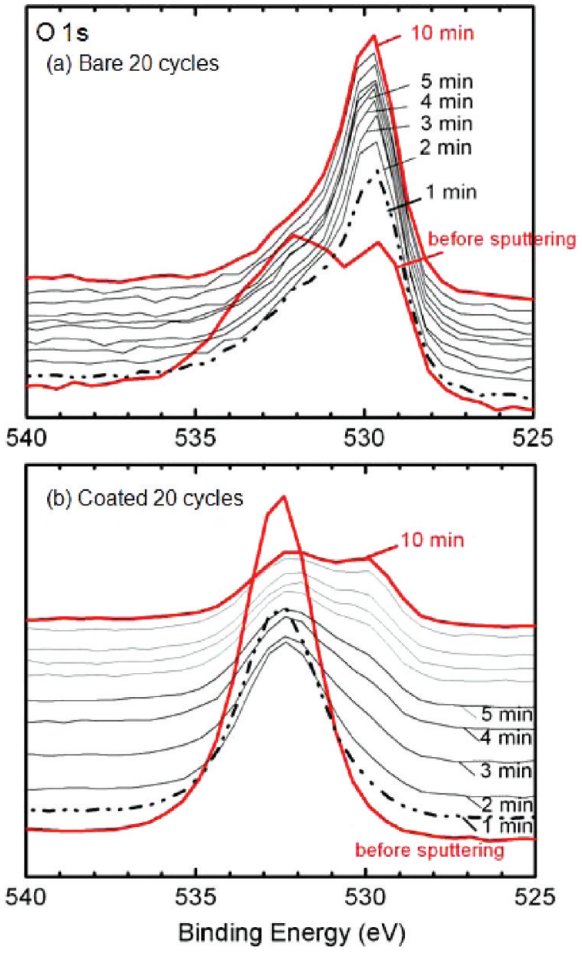

Figure 9. XPS depth profiles of the O 1s photoemission line for (a) bare "$LiCoO_2$" after 20 cycles and (b) "$AlPO_4$"-coated $LiCoO_2$ after 20 cycles.

remains on the surface of $LiCoO_2$ beneath the newly formed species.

Al 2s and Al 2p Regions. As expected, Al was not detected on the pristine and cycled bare electrodes. The Al 2s photoemission spectra of the pristine and cycled coated electrodes after subtracting the P 2p satellite contribution are shown in Figure 11. The Al 2s region of "$AlPO_4$"-coated $LiCoO_2$ powder (Figure 11a) displays a single component at 118.7 eV, which is consistent with that of $LiAlO_2$ or heavily Al-doped $LiCo_{1-y}Al_yO_2$ as reported previously.[34] The Al 2s region of the pristine coated electrode (Figure 11b) displays a highly asymmetric line, which was deconvoluted into two components. One component is at 118.6 eV, which is attributed to $LiAlO_2$ or heavily Al-doped $LiCoO_2$ (~118.7 eV).[34] The other component is at ~120.8 eV with the corresponding Al 2p line at ~75.7 eV (Figure S7b, Supporting Information). The intensity of the high-energy component for the discharged coated electrodes after 1 and 20 cycles increased at the expense of the $LiAlO_2$ component, as shown in Figure 11c, d. After 20 cycles, the $LiAlO_2$ component is no longer visible and only the high-energy component at 120.8 eV is prominent in Figure 11d. (The corresponding Al 2p line is at ~75.9 eV as shown in Figure S7d, Supporting Information). The high-energy component which appears in the coated pristine electrode, coated electrode after 1 cycle, and the entire peak in the coated electrode after 20 cycles indicates that a fraction of the Al (pristine electrode and electrode after 1 cycle) and the entire Al (electrode after 20 cycles) is present in a highly ionic bonding environment. Furthermore, such high binding energies for the Al 2s and 2p lines cannot be attributed to a pure form of aluminum oxides or hydroxides with Al 2s binding energy in the range of 117.0−119.0 eV.[34] However, such high binding energies for Al 2s and Al 2p were observed for various Al-containing fluorides, oxyfluorides, and hydroxyfluorides. For example, the Al 2s line of AlF_3 is at ~121.6 eV (reference material in this study); Al 2s and Al 2p lines for K_3AlF_6[68] are at 120.6 and 75.8 eV; the Al 2p line of Al-containing oxyfluoride (Al−O−F)[64] is ~75.8 eV, and the Al 2p line of Al-$(OH)_xF_{3-x}$[66] is ~76.0 eV. Accordingly, the Al high binding energy component can be due to surface species in the form of mixed-metal fluorides and/or oxyfluorides and/or hydroxyfluorides. It should be noted that the formation of Al-containing fluorides and/or oxyfluorides and/or hydroxyfluorides in the pristine coated electrode is consistent with results published by Edström et al.,[57] in which the authors observed a small impurity of LiF on fresh laminates (with no previous contact with the electrolyte). The authors suggested that the observed LiF was formed as a consequence of a dehydrofluorination reaction in PVDF binder, generating HF, which then reacts with the active material or Li_2CO_3 to form LiF. It is interesting to note that the entire Al in the discharged coated electrode after 20 cycles was found in the form of mixed-metal fluorides and/or oxyfluorides. It is worth noting that the low-energy component of Li(Al,Co)O_2 was not revealed after 20 min of sputtering (Figures S7e and S8, Supporting Information) indicating that the $LiCo_{1-y}Al_yO_2$ was totally consumed during cycling.

Surface Chemical Compositions. The surface chemical compositions of pristine and discharged electrodes after 1 and 20 cycles for bare and coated $LiCoO_2$ are listed in Table 2. First, the most noticeable changes in the surface chemistry of the cycled bare electrodes are the surface atomic concentrations of Li and F in the LiF and $Li_xPF_yO_z$ components, which were found to considerably increase during cycling. The surface concentration of F bound in LiF increased from 0.9 (pristine) to 5.0 (after 1 cycle) and 5.3 atom % (after 20 cycles) while that of F bound in $Li_xPF_yO_z$ increased from 0 (pristine) to 4.8 (after 1 cycle) and 7.0 atom % (after 20 cycles). The surface layers of LiF and $Li_xPF_yO_z$, which were presumably formed from the degradation of the electrolyte and side reactions between the electrolyte and Li_xCoO_2, is relatively thin as the surface concentration of the carbon black component is reduced by only about 50% relative to pristine bare electrode. Second, in contrast to the cycled bare electrode, which mainly had surface buildups of LiF and $Li_xPF_yO_z$ during cycling, considerable amounts of Co-containing and Al-containing oxyfluorides (F/Co ratios close to 1.7) were detected on the cycled

(68) McGuire, G. E.; Schweitzer, G. K.; Carlson, T. A. *Inorg. Chem.* **1973**, *12*, 2450.

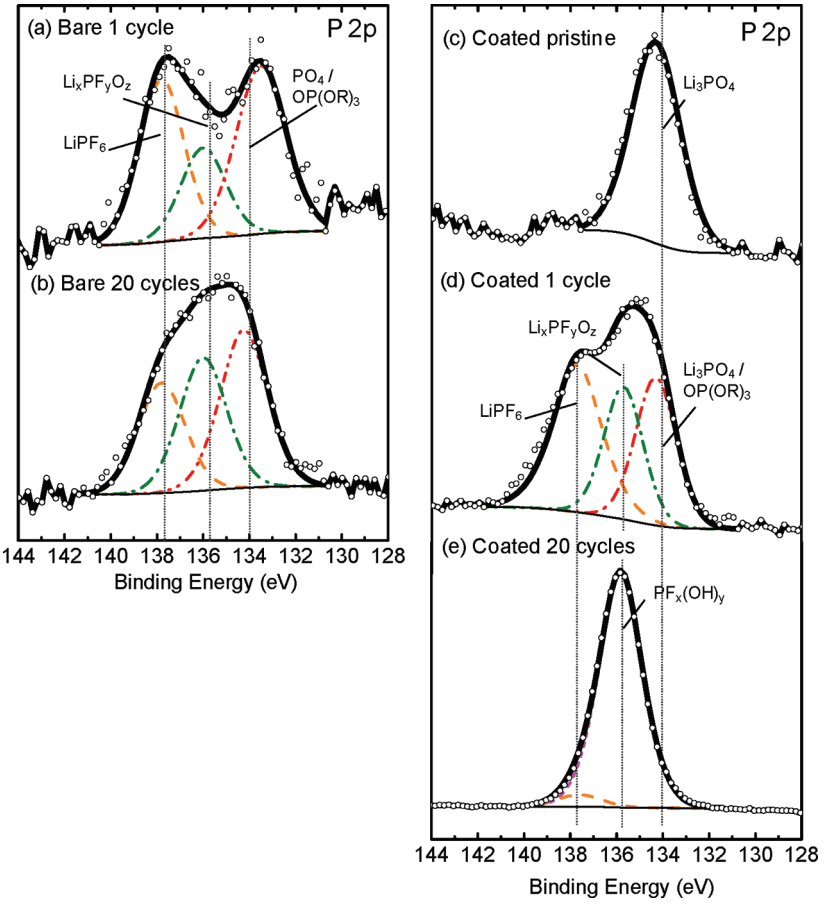

Figure 10. XPS spectra of the P 2p photoemission line for bare "$LiCoO_2$" in the condition of (a) after 1 cycle and (b) after 20 cycles and "$AlPO_4$"-coated $LiCoO_2$ in the condition of (c) pristine electrode, (d) after 1 cycle, and (e) after 20 cycles.

coated electrodes. A very small amount (barely detectable) of Co-containing oxyfluoride species was detected on the cycled bare electrodes. The surface concentrations of Co bound to oxygen atoms in pristine bare and coated electrodes were 1.4 atom % and 0.8 atom %, respectively. The surface concentrations of Co for bare electrodes did not change much during cycling (2.5 atom % after 1 cycle and 2.2 atom % after 20 cycles). In contrast, the surface concentration of Co in the pristine coated electrode of 0.8 atom % remained relatively the same after 1 cycle (~0.6 atom %) but increased to 7.4 atom % after 20 cycles. Furthermore, the surface chemistry of Co changed from the trivalent state in pristine coated $LiCoO_2$ to a divalent state in a Co-containing fluoride and/or oxyfluoride after 20 cycles. The surface concentration of Al remained relatively unchanged during cycling. However, a significant change in Al chemistry occurred during cycling. Al was present in the trivalent state but with 70% of Al bound to oxygen and 30% bound to F for the pristine coated electrode. After one cycle, roughly 27% of Al was bound to oxygen and 73% was bound to F while the entire Al was bound to F after 20 cycles. As the carbon black component in the C 1s spectrum and Li_3PO_4 component in the P 2p spectrum are no longer visible for the cycled coated electrode after 20 cycles, a relatively thick layer of metal fluorides and/or oxyfluorides was formed on the particle surface. Third, the surface concentration of P increased from 0.5 atom % (pristine coated electrode) to 1.3 atom % (after 1 cycle) and 10.5 atom % (after 20 cycles). The P 2p spectra of the coated electrode after 20 cycles showed that 95% of P was present in the pentavalent state in a hydroxyfluoride environment such as $PF_x(OH)_y$, and the remainder (5%) was due to the $LiPF_6$ in the electrolyte. The $PF_x(OH)_y$ type of species could be promoted in the presence of surface coating materials, namely, $LiAlO_2$ or heavily Al-doped $LiCoO_2$ in this study, which could provide additional hydroxyls to the coated samples. For example, AlO(OH) (Al 2s ~118.9 eV) and/or $Al(OH)_xF_{3-x}$ (Al 2s ~120.8 eV) could exist in the coated pristine electrode. Furthermore, the formation of $PF_x(OH)_y$ (e.g., $PF_3(OH)_2$) may proceed via the following reactions deduced from the previous study:[57] (1) $LiPF_6 \Rightarrow LiF + PF_5$, (2) $PF_5 + H_2O \Rightarrow PF_3O + 2HF$; $PF_3O + H_2O => PF_3(OH)_2$. It should be noted that such reaction paths need to be verified with additional experiments.

General Discussion

Proposed Mechanism of Enhanced Capacity Retention for Coated $LiCoO_2$. Figure 12 shows the proposed surface chemical compositional changes of bare and "$AlPO_4$"-coated $LiCoO_2$ during cycling to 4.7 V vs Li, from which the mechanism of enhanced capacity retention by coating is discussed. We have previously shown that the coating

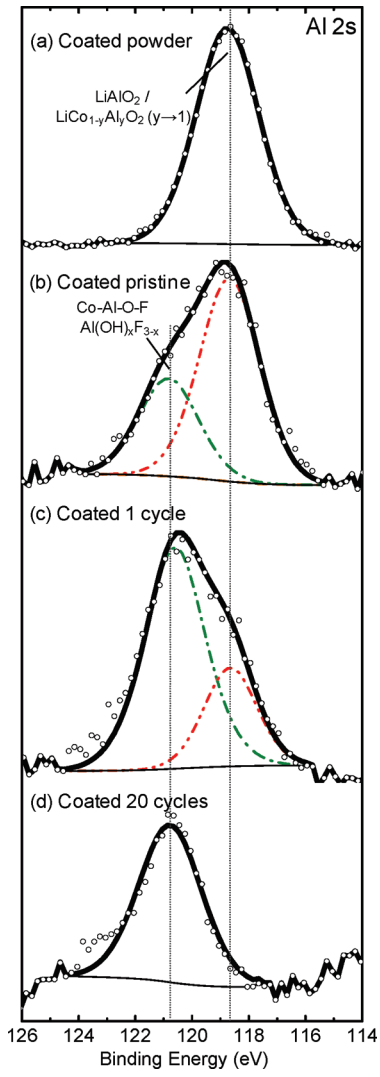

Figure 11. XPS spectra of the Al 2s photoemission line for "$AlPO_4$"-coated $LiCoO_2$ in the condition of (a) powder sample, (b) pristine electrode, (c) after 1 cycle, and (d) after 20 cycles.

material, "$AlPO_4$", consists of two major phases.[34] One is a 10 nm-thick film of Al-rich $LiCo_{1-y}Al_yO_2$ solid solution. The other is a nonuniform distribution of Li_3PO_4 with thickness up to ~100 nm. In our previous study,[34] we have reported that the amount of carbonate specie (i.e., Li_2CO_3) is reduced by about 70% for the coated $LiCoO_2$ relative to bare "$LiCoO_2$". Having more surface Li_2CO_3 on $LiCoO_2$ has been reported to lead to higher impedance growth as suggested by previous studies.[69] However, other previous studies have shown that Li_2CO_3 can readily dissolve during electrochemical cycling[28] or upon exposure to the electrolyte that typically contains a trace amount of HF.[50] In this study, we are unable to discuss the effect of having more Li_2CO_3 alone on the electrode impedance growth of bare and coated $LiCoO_2$ during cycling. The presence of the coating layer promotes the formation of Co-containing and Al-containing oxyfluorides, and species such as $PF_x(OH)_y$, as shown in Figure 12. These Co and Al-containing oxyfluorides can be formed by reactions between HF in the electrolyte and $LiCoO_2$ or $LiCo_{1-y}Al_yO_2$. Having surface Co in the form of oxyfluoride species in the cycled coated electrodes (Figure 2) is in agreement with the increasing acidity in the solid-superacid model[19,24,25] with the addition of coating materials to the electrolyte. However, this observation is in an apparent disagreement with the HF-scavenge model reported previously.[20,21] In this study, we propose that once Co-containing and Al-containing oxyfluorides and species like $PF_x(OH)_y$ were developed on the surface of the cycled coated electrodes, the following processes may take place to reduce further electrode impedance growth and enhance capacity retention relative to bare electrodes during extensive cycling. First, they can lower the Co dissolution from the cycled coated electrodes and deposition of Co-containing species on the negative electrode during subsequent cycling, where deposition of Co species is shown to increase electrode impedance.[33] Second, further degradation of $LiPF_6$ on active Li_xCoO_2 particles can be reduced relative to the bare electrode during subsequent cycling. As the molar volume of CoF_2 is two times greater than that of LiF, and a large fraction of the coated $LiCoO_2$ particle surface is covered by $PF_x(OH)_y$ like species developed on the cycled coated electrodes and Li_3PO_4 present in the original coating layer; none of active particle surface in the cycled coated electrodes is exposed to the electrolyte in comparison to a relatively large fraction of active particle surfaces in the cycled bare electrodes. This argument is different from the removal of insulating species such as Li_2CO_3 and LiOH by HF proposed in the solid-superacid model.[19,24,25] Third, oxygen loss from bulk and structural damage of active particles can be reduced by the thick surface layer as synchrotron X-ray diffraction data have revealed no noticeable changes for cycled coated electrodes but selective broadening of discharged bare electrode after 20 cycles (Figure 3). The key hypothesis in the proposed mechanism is that coating materials can promote the formation of oxyfluorides and species like $PF_x(OH)_y$ during initial charge and discharge processes, which is essential to reduce the growth of highly resistant films upon subsequent cycling. If the hypothesis were true, one can improve the cycling performance of $LiCoO_2$ to high voltages by mixing $LiCoO_2$ with coating materials such as Al_2O_3, where similar surface compositional changes on the cycled electrodes to cycled "$AlPO_4$"-coated electrodes may occur.

Test of Proposed Mechanism. To verify the hypothesis, we mixed 5 wt % γ-Al_2O_3 nanoparticles with a commercial $LiCoO_2$ (Alfa Aesar, 99.5% metals basis; the X-ray powder diffraction pattern is shown in Figure S1, Supporting Information; the surface chemistry characterization of γ-Al_2O_3 by XPS is shown in Figure S9, Supporting Information) and investigated the effects of Al_2O_3 addition on the capacity retention upon cycling to 4.7 V vs Li. Figure 13a,b shows the galvanostatic voltage profiles of a commercial bare $LiCoO_2$ electrode and an electrode consisting of the commercial $LiCoO_2$ mixed with 5 wt %

(69) Pereira, N.; Matthias, C.; Bell, K.; Badway, F.; Plitz, I.; Al-Sharab, J.; Cosandey, F.; Shah, P.; Isaacs, N.; Amatucci, G. G. *J. Electrochem. Soc.* **2005**, *152*, A114.

Table 2. Binding Energies (eV) and Atomic Percentages (%) of the Elements Li, C, O, F, P, and Co from the XPS Spectra of Bare and "$AlPO_4$"-Coated $LiCoO_2$ Electrodes before and after Cycling for 1 Cycle and 20 Cycles

		Bare electrode		Bare 1 cycle		Bare 20 cycles	
Peak	Assignments	BE(eV)	Atom%	BE(eV)	Atom%	BE(eV)	Atom%
Li 1s	$LiCoO_2$ (~54.3 eV)	54.4	2.1	54	2.8	54.0	2.3
	LiOH (55 eV) / Li_2CO_3 (55.5 eV) / LiF (56 eV) / $Li_xPF_yO_z$ / $LiPF_6$ (56.8~57 eV)	56.3	3.1	56.5	7.8	56.6	12.7
C 1s	Carbon Black (284.6 eV) / Hydrocarbon (285.0 eV) Shake-up satellite (~290.5 eV)	284.6 / 290.5	49.2	284.6 / 290.5	37.7	284.6 / 290.5	26.4
	C-O (~286.1 eV) CH_2-CF_2(PVDF) (~286.4eV)	286.2	9.0	286.2	7.2	286.3	9.2
	O-C-O / C=O (~287.6 eV)	287.6	2.6	287.6	2.8	287.6	2.5
	O-C=O (~289 eV)	288.9	1.7	288.9	1.5	288.9	2.4
	Li_2CO_3 (~290.3 eV) CF_2 (PVDF) (~290.9 eV)	290.8	4.7	290.7	4.1	290.7	4.0
	CF_3 (~293.5 eV)	293.3	0.7	293.3	0.7	292.7	1.0
O 1s	Lattice oxygen in $LiCoO_2$ (~529.8 eV)	529.8	3.0	529.5	3.6	529.5	3.3
	hydroxide group (ie:LiOH) (~531.0 eV)			531.0	2.2	531.0	0.8
	Surface oxygen in $LiCoO_2$ (~531.7 eV) / O-C=O (ie: $ROCO_2Li$) (~532.0 eV) / Carbonates (ie: Li_2CO_3) (~532.1 eV)	532.1	4.4	532.0	2.1	532.0	3.3
	$OP(OR)_3$ / O-C=O (ie: $ROCO_2Li$) (~533.5 eV)	533.6	2.2	533.5	1.8	533.5	3.1
	$Li_xPF_yO_z$ (~534.6 eV)					534.6	1.2
F 1s	LiF (~685.1 eV)	685.1	0.9	685.5	5.0	685.5	5.3
	$Li_xPF_yO_z$ (~686.6 eV)			686.6	4.8	686.6	7.0
	PVDF(CH_2-CF_2) (~688 eV) / $LiPF_6$ (~688.5 eV)	688.0	15.0	687.9	12.8	688.0	12.7
P 2p	Phosphate (ie: $OP(OR)_3$ ~134 eV)			133.5	0.2	134.2	0.4
	$Li_xPF_yO_z$ (135.5 eV~136 eV)			136.0	0.1	136.0	0.4
	$LiPF_6$ (~137.8 eV)			137.8	0.2	137.8	0.3
Co $2p_{3/2}$	$LiCoO_2$ (~780 eV)	780.1	1.4	779.9	2.5	779.8	2.2
	satellite (+~10 eV)	789.8		788.2		788.2	

		Coated pristine		Coated 1 cycle		Coated 20 cycles	
Peak	Assignments	BE(eV)	Atom%	BE(eV)	Atom%	BE(eV)	Atom%
Li 1s	$LiCoO_2$ (~54.3 eV)	54.5	1.3	54.4	1.4		
	Li_2CO_3 (55.5 eV) / LiF (56 eV) / $Li_xPF_yO_z$ / $LiPF_6$ (56.8~57 eV)	56.2	1.7	57.2	14.3	56.5	7.9
C 1s	Carbon Black (284.6 eV) / Hydrocarbon (285.0 eV) Shake-up satellite (~290.5 eV)	284.6 / 290.5	64.3	284.6 / 290.5	31.6	284.6 / 290.5	0.3
	Hydrocarbon (285.0 eV)					285.2	4.7
	C-O (~286.1 eV) CH_2-CF_2(PVDF) (~286.4eV)	286.3	3.8	286.3	4.5	286.1	1.7
	O-C-O / C=O (~287.6 eV)	287.6	2.1	287.6	2.7	287.6	1.5
	O-C=O (~289 eV)	289.0	1.2	288.9	1.2	289.0	0.5
	Li_2CO_3 (~290.3 eV) CF_2 (PVDF) (~290.9 eV)	290.8	3.4	290.8	2.7	290.3	0.3
	CF_3 (~293.5 eV)	293.3	0.4	293.3	0.5	293.0	0.1
O 1s	Lattice oxygen in $LiCoO_2$ (~529.8 eV)	529.9	2.3	529.8	1.0		
	Li_3PO_4 (~531.6 eV) / Surface oxygen in $LiCoO_2$ (~531.7 eV) / O-C=O (ie: $ROCO_2Li$) (~532.0 eV) / Carbonates (Li_2CO_3..) (~532.1 eV)	532.0	3.2	532.2	4.5		
	Co-Al-O-F(~532.7 eV) / $PF_x(OH)_y$					532.8	24.3
	$OP(OR)_3$ / O-C=O (ie: $ROCO_2Li$) (~533.5 eV)	533.6	1.4	533.4	3.2		
	$Li_xPF_yO_z$ (~534.6 eV)			534.7	1.7		
F 1s	LiF (~685.1 eV)	685.1	0.6	685.5	3.3		
	Co-Al-O-F (CoF_2 ~686.0 eV)					686.1	12.0
	$Li_xPF_yO_z$ (~686.6 eV)			686.7	10.7		
	PVDF(CH_2-CF_2) (~688 eV) / $LiPF_6$ (~688.5 eV) / $PF_x(OH)_y$	687.9	11.5	688.0	14.0	688.5	27.9
P 2p	Phosphate (ie: $OP(OR)_3$ ~134 eV)	134.3	0.5	134.3	0.4		
	$Li_xPF_yO_z$ (135.5 eV~136 eV) $PF_x(OH)_y$			135.7	0.4	135.8	10.0
	$LiPF_6$ (~137.8 eV)			137.7	0.5	137.6	0.5
Al 2s	$LiAl_yCo_{1-y}O_2$ (y~1)(~118.7 ev)	118.7	0.7	118.7	0.3		
	Co-Al-O-F (K_3AlF_6~120.6 ev) / $Al(OH)_xF_{3-x}$	120.8	0.3	120.6	0.8	120.8	1.0
Co $2p_{3/2}$	$LiCoO_2$ (~780 eV)	780.3	0.8	780.5	0.6		
	satellite (+~10 eV)	790.1		788.6			
	Co-Al-O-F (CoF_2 ~783.7 eV)					783.1	7.4
	satellite (+~6 eV)					788.3	

γ-Al_2O_3 nanoparticles (< 50 nm, Sigma-Aldrich), respectively. These test conditions included a C/5 rate (bare: 0.24 mA/cm^2, mixed: 0.25 mA/cm^2) and cycling between voltage limits of 2.5 and 4.7 V vs Li for 40 cycles. It is remarkable to note that the cell with a mixture of commercial $LiCoO_2$ and Al_2O_3 exhibits better capacity retention and smaller polarization upon cycling relative to commercial bare $LiCoO_2$. Below we compare the changes in the surface compositions of cycled Li_xCoO_2 electrode with and without Al_2O_3 with those of bare and coated electrodes discussed above.

The surface chemical compositions of the commercial bare $LiCoO_2$ electrode and the mixed electrode of $LiCoO_2$ and Al_2O_3 before and after cycling were analyzed by XPS. The Co 2p and Al 2s spectra are shown in Figure 14. Co 2p spectra in Figure 14a show that the surface of the mixed electrode after 40 cycles exhibits only one component corresponding to Co-containing fluorides and/or oxyfluorides (~3.4 atom %) while the cycled commercial bare $LiCoO_2$ electrode shows that some surface Co ions are bound to fluorine (~2.0 atom %) and others are bound to oxygen in $LiCoO_2$ (~0.7 atom %). These Co-containing fluoride and/or oxyfluoride species on the cycled commercial and mixed electrodes can be removed by sputtering for 3 and 6 min, respectively. A higher amount of Co-containing fluoride and/or oxyfluoride species was detected on the commercial bare electrodes after 40 cycles relative to the bare electrodes after 20 cycles. This difference may be attributed to the facts that

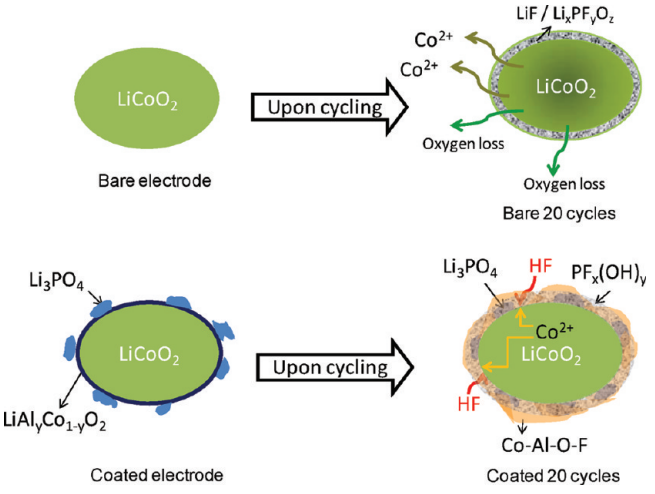

Figure 12. Proposed working mechanism of "$AlPO_4$"-coated $LiCoO_2$. The Al substituted solid-solution layer reacts with HF and traps dissolved Co ion from the bulk. The coating materials reduce further Co dissolution as well as surface reactions between active particles and electrolyte by forming the "Co−Al−O−F" type of thin film on the surface. In contrast, the bare "$LiCoO_2$" particles are exposed to and react with the electrolyte, continuously to form highly resistant decomposition product of electrolyte, and then isolate the active particle. Co dissolution and oxygen loss also lead to structural instabilities such as formation of the stacking fault.

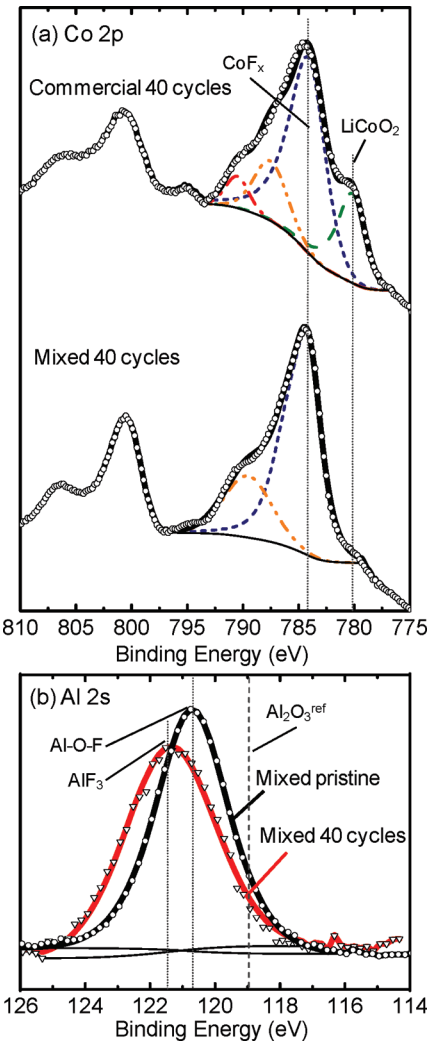

Figure 14. XPS spectra of (a) Co 2p and (b) Al 2s for cycled commercial bare $LiCoO_2$ and commercial bare $LiCoO_2$ mixed with 5 wt % Al_2O_3 in the discharged state after 40 cycles.

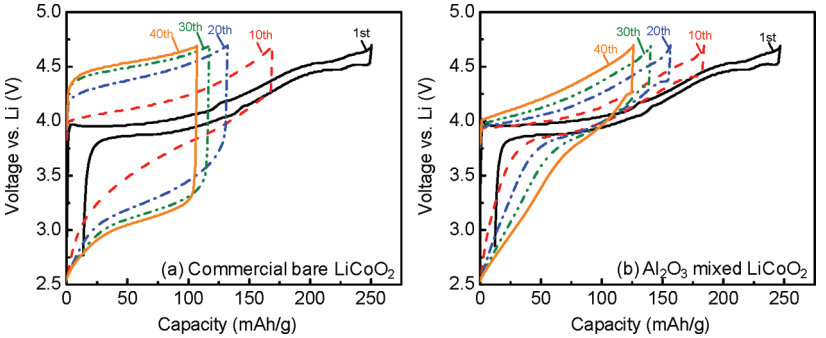

Figure 13. Voltage profiles of (a) commercial bare $LiCoO_2$ and (b) commercial bare $LiCoO_2$ mixed with 5 wt % Al_2O_3 during cycling between 2.5 and 4.7 V at a C/5 rate for 40 cycles.

the cycling conditions are not exactly identical, and the commercial $LiCoO_2$ is less lithium overstoichiometric than bare "$LiCoO_2$", as evidenced by observed phase transitions in the voltage profile in Figure 13a. In addition, the Al 2s spectrum of the cycled mixed electrode after shifts to higher binding energy relative to the pristine electrode is shown in Figure 14b. The peak at 121.4 eV can be attributed to aluminum ions in fluorides based on the binding energy of AlF_3 (~121.6 eV). It should be noted that the binding energy for the Al 2s of the pristine mixed electrode (~120.7 eV) was found ~1.7 eV higher than that of γ-Al_2O_3 powder (~119.0 eV). This peak is likely due to aluminum ions in a fluorine and oxygen environment, which can result from a chemical interaction between Al in γ-Al_2O_3 powder and the fluorine in PVDF as discussed previously. These observations suggest that not only coated $LiCoO_2$ but also adding Al_2O_3 in the $LiCoO_2$ electrode lead to increased surface coverage of Co- and Al-containing fluoride and/or oxyfluoride species during cycling, which can prevent further Co dissolution and side reactions between the electrolyte and the active material and reduce impedance growth during cycling to high voltages. The detailed mechanism on how the fluoride and/or oxyfluoride species stabilizes active materials and affects the electrode impedance characteristics during cycling is not understood, which will be examined in future studies.

Conclusions

SEM and XPS studies have shown that the surface morphological and chemistry changes of cycled bare and coated electrodes are considerably different. A very thin surface layer that predominately consists of LiF and $Li_xPF_yO_z$ grows during cycling of the bare electrode and partially covers the surfaces of active particles. In contrast, a thick surface layer primarily includes Co- and Al- containing fluorides and/or oxyfluorides and PF_x-$(OH)_y$-like species, which completely covers the surfaces of Li_xCoO_2. It is hypothesized that Al-containing oxides on the surfaces of coated $LiCoO_2$ particles promote the formation of Co−Al−O−F species on the particle surfaces. It is proposed that these surface species serve to protect active particles from further side reactions with the electrolyte, possibly prevent bulk oxygen loss as suggested by synchrotron X-ray diffraction data, and reduce impedance growth relative to cycled bare electrodes during cycling to high voltages. This hypothesis is further supported by an experiment, which shows that addition of Al_2O_3 powder to $LiCoO_2$ leads to enhanced stability and reduced electrode impedance growth upon cycling, where similar electrode surface chemistry changes during cycling have been found to cycled "$AlPO_4$"-coated electrodes.

Acknowledgment. This work was supported in part by the MRSEC Program of the National Science Foundation under Award No. DMR 02-13282 and the Assistant Secretary for Energy Efficiency and Renewable Energy, Office of Freedom CAR and Vehicle Technologies of the U.S. Department of Energy under Contract No. DE-AC03-76SF00098 with the Lawrence Berkeley National Laboratory. The authors would like to thank J. Cho for providing bare and coated $LiCoO_2$ samples, A. Appapillai for collecting the electrochemical cycling data shown in Figures 1a,b and S2, and S. Chen for the assistance in SEM imaging. The synchrotron diffraction experiments were made possible through the support of the Japanese Ministry of Education, Science, Sports and Culture, Nanotechnology Support Project (Proposal No. 2007B/BL02B2) with the approval of Japan Synchrotron Radiation Research Institute (JASRI).

Supporting Information Available: X-ray diffraction patterns for reference compounds; open-circuit voltages; XPS Li 1s spectra; reference XPS C 1s spectra for Super P carbon powder, PVDF powder and 50 wt % carbon + 50 wt % PVDF composite electrode; comparison of the satellite relative area of Co $2p_{3/2}$ and Co 3p spectra; reference XPS F 1s and O 1s spectra for 50 wt % carbon + 50 wt % PVDF composite electrode; XPS Al 2p spectra; XPS Al 2s spectra for coated electrode in the condition of 20 cycles after sputtering for 20 min; and XPS Al 2s and O 1s spectra for γ-Al_2O_3 (PDF). This material is available free of charge via Internet at http://pubs.acs.org.